Tectonophysics 608 (2013) 929–946

Contents lists available at ScienceDirect

Tectonophysics

journal homepage: www.elsevier.com/locate/tecto

A late Archean tectonic mélange in the Central Orogenic Belt, North China Craton

Junpeng Wang [a,b], Timothy Kusky [b,c,*], Ali Polat [b,d], Lu Wang [b], Hao Deng [a], Songjie Wang [a]

[a] Faculty of Earth Sciences, China University of Geosciences, Wuhan 430074, China
[b] State Key Laboratory of Geological Processes and Mineral Resources, China University of Geosciences, Wuhan 430074, China
[c] Three Gorges Research Center for Geo-hazards, Ministry of Education, China University of Geosciences, Wuhan 430074, China
[d] Department of Earth and Environmental Sciences, University of Windsor, Windsor, ON N9B 3P4, Canada

ARTICLE INFO

Article history:
Received 18 January 2013
Received in revised form 9 July 2013
Accepted 20 July 2013
Available online 31 July 2013

Keywords:
Late Archean
Tectonic mélange
Zanhuang Massif
Central Orogenic Belt
North China Craton

ABSTRACT

Laterally extensive belts of mélange characterize Phanerozoic convergent plate margins, but are rare in Archean terranes. We document a late Archean mélange in the Zanhuang Massif of the North China Craton (NCC). The Zanhuang mélange separates a passive margin to foreland basin sequence developed on the western edge of the Eastern Block of the NCC from an arc terrane consisting of trondhjemitic, tonalitic and granodioritic (TTG) gneisses in the Central Orogenic Belt (COB) of the NCC. The mélange belt contains a structurally complex tectonic mixture of metapelites, metapsammites, marbles and quartzites mixed with exotic tectonic blocks of ultramafic and metagabbroic rocks, metabasalts that locally include relict pillow structures, and TTG gneisses. All units in the mélange have been intruded by mafic dikes that were subsequently deformed, and are now preserved as garnet–amphibolite boudins. We interpret the mélange to mark the suture zone between the Eastern Block and the arc terrane in the COB. Field relationships and geochemistry suggest that the exotic ultramafic–metagabbroic–metabasaltic blocks are possible slivers of an intra-oceanic arc or fore-arc ophiolite incorporated into the mélange during the arc–continent collision process. A circa 2.5 Ga granitic pluton intrudes the mélange and undeformed circa 2.5 Ga pegmatites cut the mélange. Tectonic models for the evolution of the COB are varied, but include models that favor collision at 2.5 Ga, 2.1 Ga, and 1.8 Ga. This work shows clearly, from field structural relationships and geochronology, that the first collision must have occurred prior to 2.5 Ga, consistent with late Archean suturing of the western margin of the Eastern Block with an arc terrane (Fuping terrane) during an arc–continent collision. The presence of an Archean mélange with exotic blocks in a suture zone between an Archean arc and continental margin is clear evidence for the operation of plate tectonics at circa 2.5 Ga.

Published by Elsevier B.V.

1. Introduction

Tectonic mélanges are one of the hallmark units of Phanerozoic convergent plate boundaries and suture zones (Cawood et al., 2009; Faghih et al., 2012; Kimura et al., 2012; Kitamura and Kimura, 2012; Kusky and Bradley, 1999; Kusky et al., 1997; Wakabayashi and Dilek, 2011). The paucity of well-documented mélanges in Archean terranes has been used to suggest that plate tectonics did not operate, or operated differently in the Archean than in younger geological times (Moyen and van Hunen, 2012). In this paper, we document a well exposed Archean mélange along the tectonic boundary between two major tectonic blocks in the North China Craton (NCC), and discuss its implications for the tectonic evolution of the NCC and Archean tectonics in general.

In a general sense, the NCC is divided into the Archean Eastern Block (EB) and Western Block (WB), separated by the Central Orogenic Belt (COB, also known as the Central Domain, or Trans North China Orogen) (Figs. 1A and 2A; Kusky and Li, 2003; Kusky et al., 2001, 2004, 2007a,b; Liu et al., 2004, 2005, 2006; Polat et al., 2005, 2006b; Santosh, 2010; Zhao, 2001; Zhao et al., 1999a, 2001a,b, 2002a, 2005). Other models for the divisions of the NCC include several other microblocks within the Eastern and Western blocks, separated by circa 2.7 and 2.5 Ga greenstone belts (Li et al., 2010; Zhai, 2004; Zhai and Liu, 2003; Zhai and Santosh, 2011).

The geometry, patterns of collision and timing of amalgamation of the NCC have been debated for several decades, largely because of a paucity of reliable structural analyses coupled with dating of specific tectonic events. Four mainly different models have been proposed to account for the controversial issues. (1) The first model is based mainly on geochronology and metamorphic P–T paths, and proposes that the Eastern Block and Western Block formed separately in the Archean, and collided (continent–continent collision) at circa 1.85 Ga above an east-dipping subduction zone, and an active margin was formed on the western margin of the Eastern Block for 650 Ma between 2.5 and

* Corresponding author at: State Key Laboratory of Geological Processes and Mineral Resources, China University of Geosciences, Wuhan 430074, China. Tel.: +86 189 7157 9211.
E-mail address: tkusky@gmail.com (T. Kusky).

0040-1951/$ – see front matter. Published by Elsevier B.V.
http://dx.doi.org/10.1016/j.tecto.2013.07.025

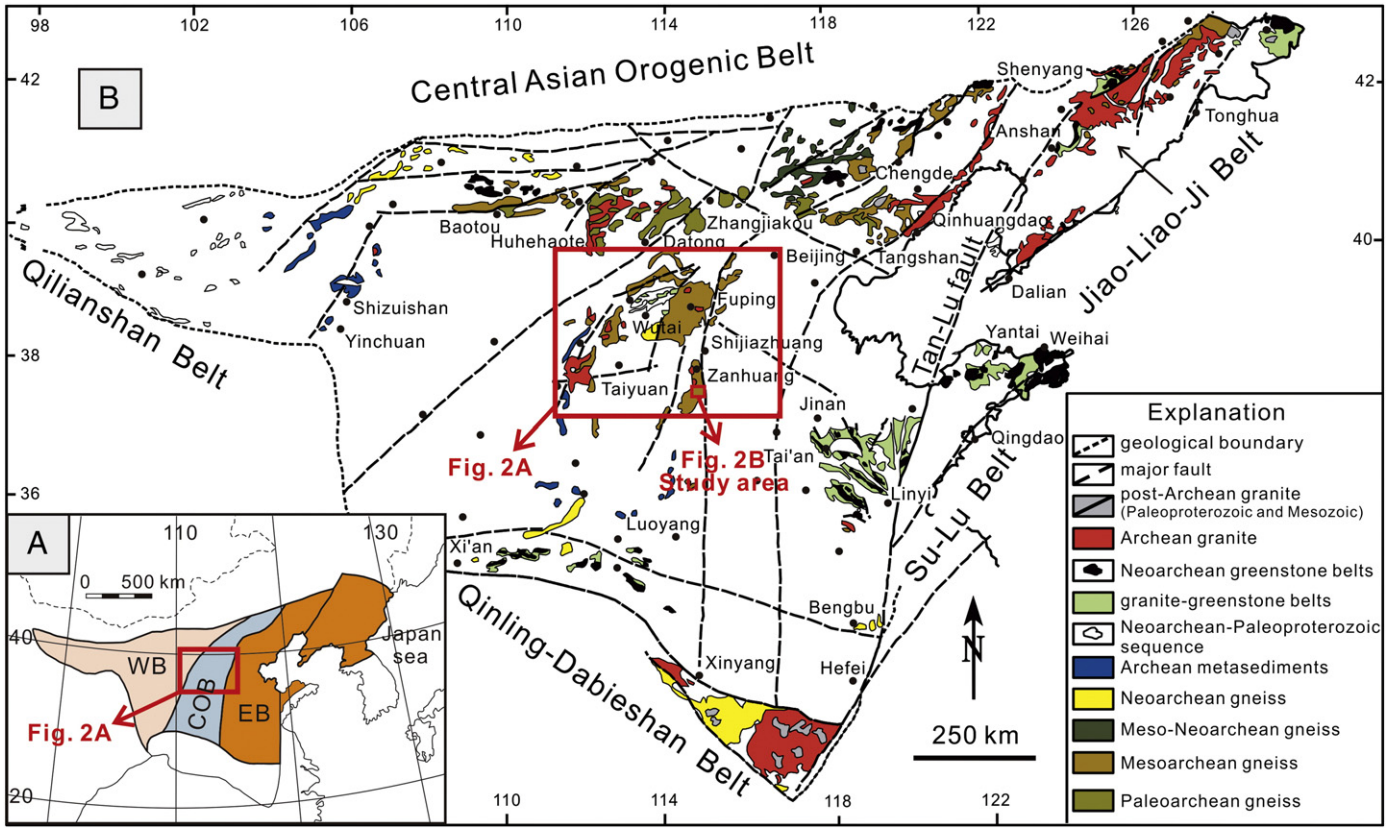

Fig. 1. A: Simplified map of the North China Craton showing the three-fold subdivision including Western Block (WB), Central Orogenic Belt (COB) and Eastern Block (EB). Map modified from Trap et al. (2009a) and Zhao et al. (2001a). B: Geological map of the North China Craton showing the distribution of major types of Precambrian rocks, and the location of the study area (Fig. 2B). Modified from Kusky and Li (2003) and Shen et al. (1992, 1994).

1.85 Ga (Kröner et al., 2005, 2006; Wilde et al., 2002; Zhang et al., 2007; Zhao et al., 1998, 1999a,b, 2000a,b, 2001a,b, 2002b, 2004, 2005, 2007, 2010). (2) The second model suggests that the Eastern Block collided with an arc (arc–continent collision) at 2.5 Ga with westward-directed subduction (Kusky, 2011a,b; Kusky and Li, 2003, 2010; Kusky and Santosh, 2009; Kusky et al., 2001, 2004, 2007a,b; Li and Kusky, 2007; Polat et al., 2005, 2006a,b), and is based on structural and lithological zonations of Archean rocks including the recognition of a foreland basin on the western margin of Eastern Block, the presence of circa 2.5 Ga accreted arc and ophiolitic fore-arc rocks. Seismic reflectors show west-dipping paleosubduction zones (Kusky, 2011a,b; Zheng et al., 2009). In this model, the 1.85 Ga deformation and metamorphism is linked to accretion of the NCC to the Columbia supercontinent along the northern margin of the NCC (Kusky, 2011a,b; Kusky and Santosh, 2009; Kusky et al., 2007b). (3) A third model invokes the Proto-North China Ocean, which formed in the COB prior to circa 2565 Ma (Wang, 2009; Wang et al., 2004, 2010), and is based on the geochemistry and structural studies of the Wutai greenstone belt and mafic–ultramafic intrusions in the Hengshan area. In this model, a magmatic arc represented by the Wutaishan granitoids, formed between 2565 and 2540 Ma in response to northwestward intra-oceanic subduction and subsequently rifted forming a back-arc basin. This model suggests that the final collision between the Eastern and Western Blocks occurred at 1.9–1.8 Ga. (4) A fourth model (Faure et al., 2007; Trap et al., 2007, 2008, 2009a,b, 2012) proposes two collisions in the COB, one at 2.1 Ga and another at 1.88 Ga but recognizes an earlier undated deformation event. Clearly, important disagreement still exists on the patterns of collision, timing of amalgamation and subduction polarity.

In this contribution we use field mapping, structural relationships, and U–Pb geochronology to document that a sequence of clastic and metacarbonate sediments deposited on the western margin of the Eastern Block of the NCC was structurally juxtaposed with an arc-like TTG terrane in the COB before 2.5 Ga. A well-preserved accretionary mélange terrane between the arc and the Eastern Block continent formed during the convergence and collision of these terranes before 2.5 Ga, based on the ages of cross-cutting undeformed intrusive pegmatites and granitic plutons that cut the structural fabrics in the mélange. This study has important implications for interpreting the different tectonic models for the evolution of the NCC mentioned above, and shows clearly that the Eastern Block and an arc terrane (Fuping terrane) in the COB collided, forming an extensive mélange belt, prior to circa 2.5 Ga.

2. Geologic background

The Archean NCC is about 1.7 million km^2 and located in the northern part of eastern China (Fig. 1A). It is surrounded by the Qilianshan and Qinling–Dabieshan Belt to the southwest, the Central Asian Orogenic Belt to the north, and the Su-Lu and Jiao-Liao-Ji Belt to the southeast (Fig. 1B; Bai and Dai, 1996; Kusky, 2011b; Kusky et al., 2007a). Major lithological units include Archean gneiss, granite and greenstone belts, 2.40 to 1.90 Ga Paleoproterozoic sequences, and 1.85 to 1.40 Ga Mesoproterozoic metasediments of Changcheng Series that overlie the Archean units (Fig. 1B; Kusky, 2011b; Kusky and Li, 2003; Kusky et al., 2007a; Li et al., 2000a,b; Meng et al., 2011).

The COB is defined as an Archean orogen based on its boundaries with Archean structures and different litho-tectonic belts (Kusky, 2011b; Kusky and Li, 2003; Kusky et al., 2007a). The COB is different from the Trans North China Orogen (TNCO) that is defined as a Paleoproterozoic orogen (Zhao et al., 2001a), even though its boundaries are Mesozoic structures (Kusky, 2011b). Generally, the COB is described to record the

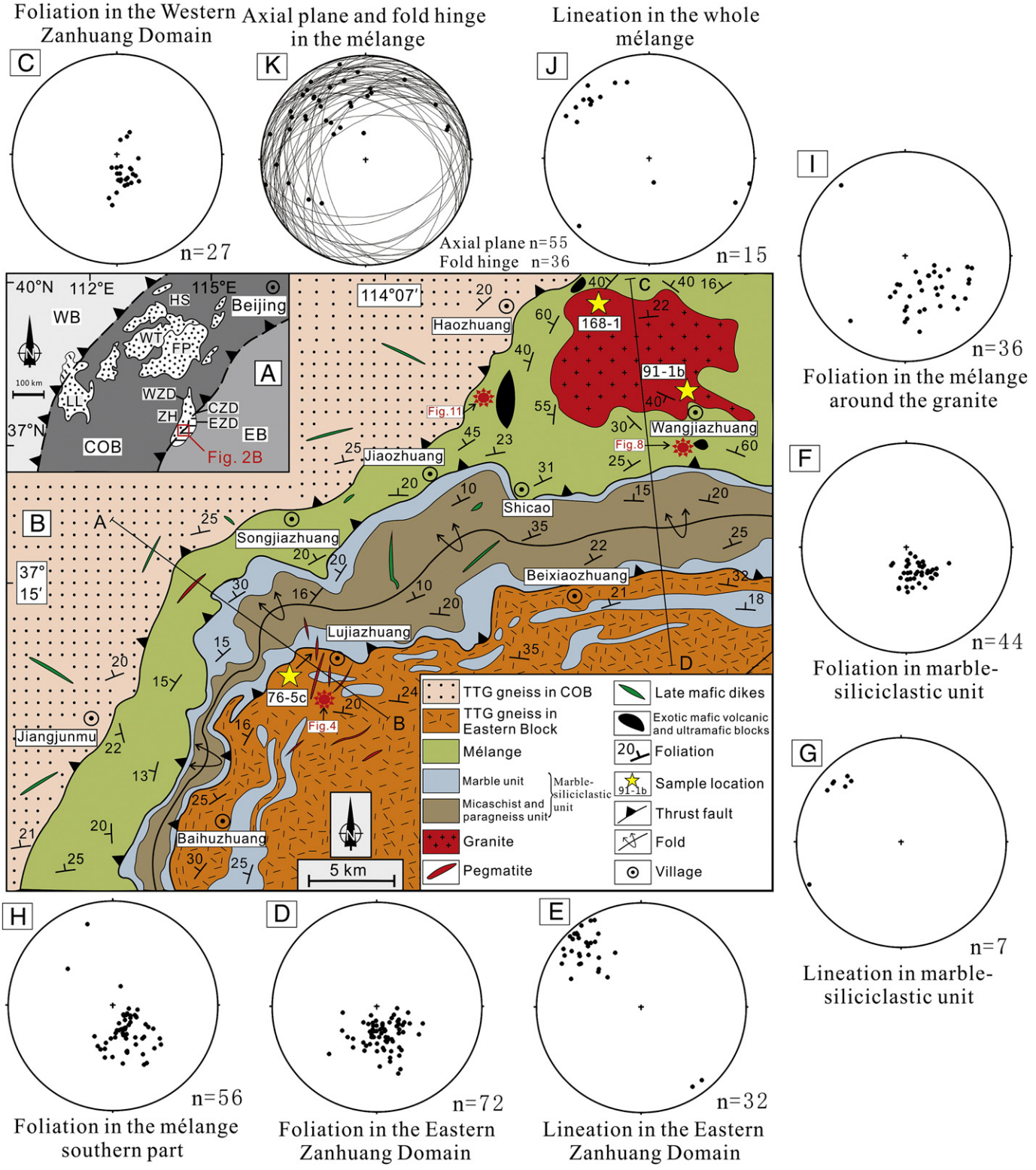

Fig. 2. A: A simple geological map of the central part of the North China Craton (NCC), showing Western Block (WB), Eastern Block (EB) and Central Orogenic Belt (COB), different massifs (Hengshan Massif = HS; Wutaishan Massif = WT; Fuping Massif = FP; Lüliangshan Massif = LL; Zanhuang Massif = ZH) within COB, and Western Zanhuang Domain (WZD), Central Zanhuang Domain (CZD), and Eastern Zanhuang Domain (EZD) of Zanhuang Massif. Map location shown in Fig. 1, and modified after Trap et al. (2009a). The thrusts dipping to the northwest are interpreted as two suture zones by Faure et al. (2007), Kusky (2011a,b) and Trap et al. (2009a). B: Geological map of the study area, showing different units of the study area, including the TTG gneisses of the COB and Eastern Block, the mélange belt, marble unit and micaschist and paragneiss unit of the marble-siliciclastic unit, the mélange is intruded by a granitic pluton with surrounding schist, marble, quartzite and volcanic rocks and cross-cut by undeformed pegmatites. The mélange belt corresponds to the southeastern (Taihang) suture in panel A. Map modified after HBGMR (1996). C–K: Equal area, lower hemisphere Schmidt diagrams of the different structural elements recognized in all different units in the study area, including the TTG gneisses of the Western Zanhuang Domain, the TTG gneisses of the Eastern Zanhuang Domain, the marble-siliciclastic unit and the Zanhuang mélange unit.

amalgamation of two main tectonic blocks, called the Eastern Block and the Western Block, to form the North China Craton's basement (Figs. 1A and 2A; Guo et al., 2002, 2005; Kröner et al., 2005, 2006; Kusky and Li, 2003; Kusky et al., 2007a; Li and Kusky, 2007; Polat et al., 2005, 2006a, b; Trap et al., 2009a; Wilde and Zhao, 2005; Wilde et al., 2002; Zhang et al., 2007; Zhao and Cawood, 2012; Zhao et al., 1998, 2001a, 2005). However, recent work suggests that there may be intervening terranes, and possibly several collisions of different ages, as described above (see review by Kusky, 2011b). From the central to southern parts of the COB, the rocks crop out in Hengshan Massif (HS), Wutaishan Massif (WT), Fuping Massif (FP), Lüliangshan Massif (LL) and Zanghuang Massif (ZH) (Fig. 2A). TTG gneiss, granite, and greenschist to granulite facies supracrustal sequences are exposed in the COB. Greenschist to amphibolite and amphibolite to granulite facies metamorphism predominates in the southeastern and northwestern parts of the COB, respectively (Kusky, 2011b; Kusky et al., 2007b; Li et al., 2000b; Zhao et al., 2001a,b). Sedimentary rocks deposited in foreland basin to cratonic platform and graben environments overlie the COB in many places (Kusky, 2011b; Kusky and Li, 2003; Kusky et al., 2007b). The circa 2.5–2.4 Ga and 1.9–1.7 Ga mafic dike swarms that experienced subsequent deformation intrude many rock types of the COB (Kröner et al., 2006; Kusky, 2011b; Kusky and Li, 2003; Kusky et al., 2007b; Peng et al., 2007; Wang et al., 2008; Xiao and Wang, 2011).

The Zanhuang Massif located on the eastern-most margin of the central and southern section of the COB (Fig. 2A) is one of the most important areas to clarify the structural and age relationships of the early convergent and collisional orogenesis between the Eastern and Western Blocks and any intervening arc or accretionary terranes. The Zanhuang Massif consists of three tectonically juxtaposed domains: Western Zanhuang Domain (WZD), Central Zanhuang Domain (CZD) and Eastern Zanhuang Domain (EZD) (Fig. 2A; Trap et al., 2009a). Trap et al. (2009a) described the Central Zanhuang Domain as a suture zone that represents the remnants of an oceanic basin separating the Fuping terrane from the Eastern Block. The Central Zanhuang Domain is a unique terrane in that it contains a well preserved Precambrian accretionary complex and mélange, with numerous exotic and native blocks tectonically dispersed in marble and siliciclastic matrices (Kusky, 2011a,b; Kusky and Li, 2003). Two cross-sections (Fig. 3; A–B and C–D) based on field relationships

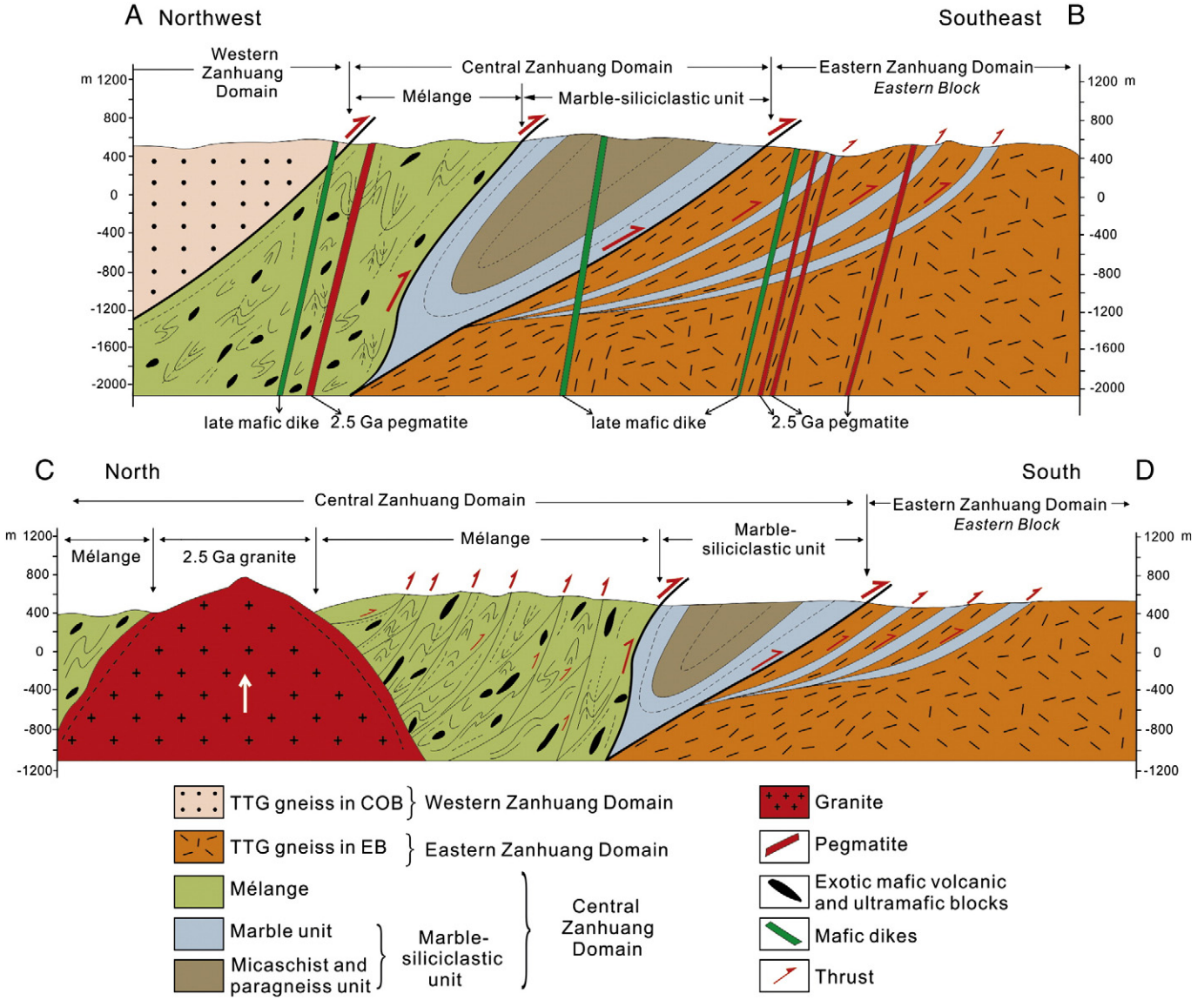

Fig. 3. Two interpretive cross-sections (A–B and C–D) through Western Zanhuang Domain, Central Zanhuang Domain to Eastern Zanhuang Domain. Note that the Western Zanhuang Domain was thrust to the southeast upon the Central Zanhuang Domain including the mélange unit and the marble-siliciclastic unit, and the Central Zanhuang Domain was thrust to the southeast upon the Eastern Zanhuang Domain. Circa 2.5 Ga granitic pluton and pegmatite intrude the Zanhuang mélange and late mafic dikes cross-cutting all units of the study area. Profile locations shown in Fig. 2B, maps modified after HBGMR (1996).

and our geological mapping show the different units and structures from the Western Zanhuang Domain, Central Zanhuang Domain to the Eastern Zanhuang Domain in the study area (Figs. 2B and 3).

The Western Zanhuang Domain consisting of TTG gneisses was thrust upon the Central Zanhuang Domain which was in turn thrust upon the Eastern Zanhuang Domain (Fig. 3; Trap et al., 2009a; Wang et al., 2003). The Central Zanhuang Domain is mainly composed of mélange units and a marble-siliciclastic unit. The highly sheared and deformed mélange units with mafic intrusions were thrust upon the marble-siliciclastic unit developed on the western edge of the Eastern Zanhuang Domain (Fig. 3). The marble-siliciclastic unit is mainly composed of a marble unit, and a micaschist and paragneiss unit. The marble unit outlines a regional synformal structure with the micaschist and paragneiss unit preserved as the core of the synform (Fig. 3). A late granitic pluton and undeformed pegmatites intrude into the mélange unit with cross-cutting structures (Fig. 3). Slices of marble unit are tectonically intercalated and imbricated in the TTG gneisses of the Eastern Zanhuang Domain (Fig. 4) defining a foreland fold-thrust belt between the marble-siliciclastic unit and the Eastern Zanhuang Domain (Figs. 2 and 3). The following section describes the litho-tectonic units of the study area in detail.

3. Litho-tectonic units of study area

3.1. TTG gneiss of the Western Zanhuang Domain in the COB

The Zanhuang mélange separates the Western and Eastern Zanhuang Domains (Figs. 2B and 3). The Western Zanhuang Domain is mainly composed of deformed TTG gneisses that experienced a partial melting episode (Trap et al., 2009a). The protolith of the gneisses, predominantly tonalite, has undergone intense metamorphism, deformation and anatexis and is intimately associated with melanocratic dioritic gneiss and leucocratic trondhjemitic veins (HBGMR, 1996; Yang et al., 2013).

The tonalitic gneiss is gray, medium-grained and granoblastic in texture, and has a SHRIMP zircon U–Pb age of circa 2692 ± 12 Ma (Yang et al., 2013). The mineral assemblage includes biotite, plagioclase and quartz, with minor epidote, muscovite and chlorite, accessory zircon, apatite and magnetite (Yang et al., 2013). The tonalitic gneiss has high SiO_2 (68–73 wt.%) and Al_2O_3 (ca. 15 wt.%) contents, and is rich in Na_2O (ca. 5 wt.%) and has low K_2O (<2 wt.%). It has high contents of Ba and Sr, low contents of Yb and Y with high Sr/Y ratios and depletion in Nb, Ta and Ti (Yang et al., 2013). On chondrite-normalized diagrams, they are characterized by fractionated rare earth element (REE) patterns and minor positive Eu anomalies (Yang et al., 2013). The tonalitic gneiss is interpreted to have been generated from partial melting of subducted oceanic crust with many similarities to high-Si adakitic rocks (Yang et al., 2013).

Minor metamorphic dioritic porphyry, amphibole schist, mafic dikes and deformed amphibolite are present in the gneisses (HBGMR, 1989, 1996). The dioritic gneiss is interpreted to have been derived from a subduction environment (Yang et al., 2013). Metamorphic temperatures and pressures of the garnet-bearing TTG gneisses from the Western Zanhuang Domain are estimated to be between 550–700 °C and 5–10 kbar based on garnet-amphibole and garnet-biotite metamorphic equilibria (HBGMR, 1989; Trap et al., 2009a). The gneisses structurally overlie the western side of the Zanhuang mélange (Figs. 2B and 3).

3.2. TTG gneiss of the Eastern Zanhuang Domain in the Eastern Block

The southeast part of the study area is the Eastern Zanhuang Domain of the Eastern Block (Figs. 2B and 3), which is composed of high-grade metamorphic TTG gneisses that are structurally distinct from the gneisses of the Western Zanhuang Domain (Trap et al., 2009a). The rocks in the Eastern Zanhuang Domain experienced amphibolite to granulite facies metamorphism (Trap et al., 2009a). No recent geochronological or thermo-barometric constraints are available although the protolith ages for the TTG gneisses are estimated to be late Archean (HBGMR, 1989, 1996; Trap et al., 2009a; Wang et al., 2003). The large ion lithophile element (LILE) contents are much higher in the Eastern Zanhuang Domain than those in the TTG gneisses of the Western Zanhuang Domain, suggesting a different petrogenetic origin. These gneisses display stronger LREE fractionation than HREE on chondrite-normalized diagrams (HBGMR, 1996). The petrology, mineralogy and geochemical characteristics suggest that the protolith of the gneisses in the Eastern Zanhuang Domain is predominantly granodiorite (HBGMR, 1996). Many tectonic slices of marble and amphibolite are

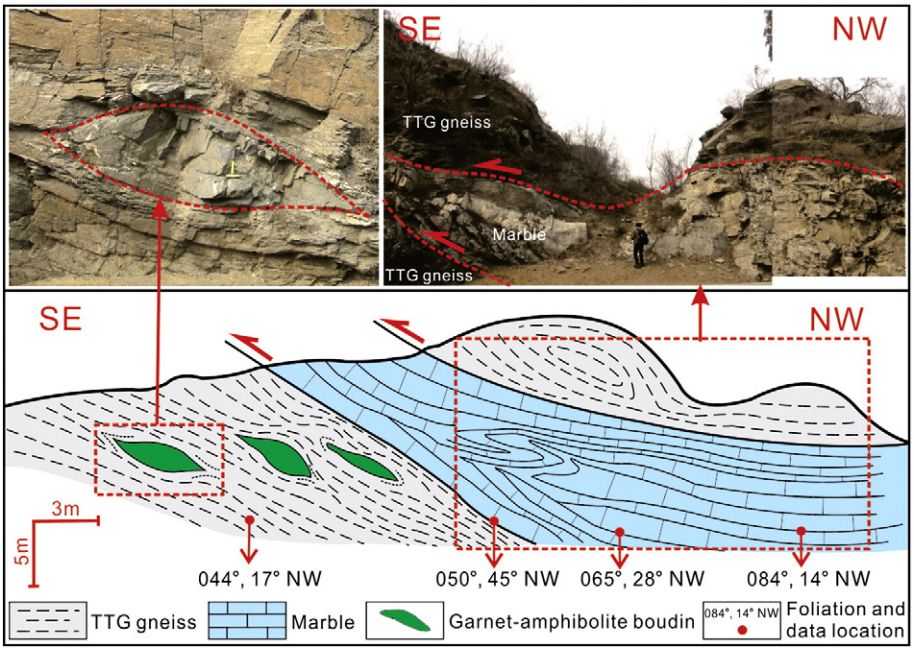

Fig. 4. Simplified sketch of structural contact between TTG gneisses of the Eastern Zanhuang Domain and the marble unit. Note that marble is strongly folded and thrust upon the gneiss, and garnet-amphibolite boudins are preserved in the TTG gneisses. Outcrop shown in Fig. 2B, near Lujiazhuang village (N37°12′50″/E114°7′26″). The data show the strike and dip angle of the foliation.

enclosed within the gneisses in the Eastern Block with clearly deformed contacts and foliations that are subparallel to the foliation in the gneisses (Figs. 2B, 3 and 4).

3.3. Marble-siliciclastic unit

The marble-siliciclastic unit is located along the western margin of the Eastern Zanhuang Domain of the Eastern Block. From east to west, two litho-tectonic units can be recognized with a subparallel distribution: (i) marble unit and (ii) micaschist and paragneiss unit (Fig. 2B and 3).

3.3.1. Marble unit

The marble unit forms two main belts, outlining a large synformal structure of the micaschist and paragneiss unit and marble unit (Figs. 2B and 3). One of the marble belts is located at the western margin

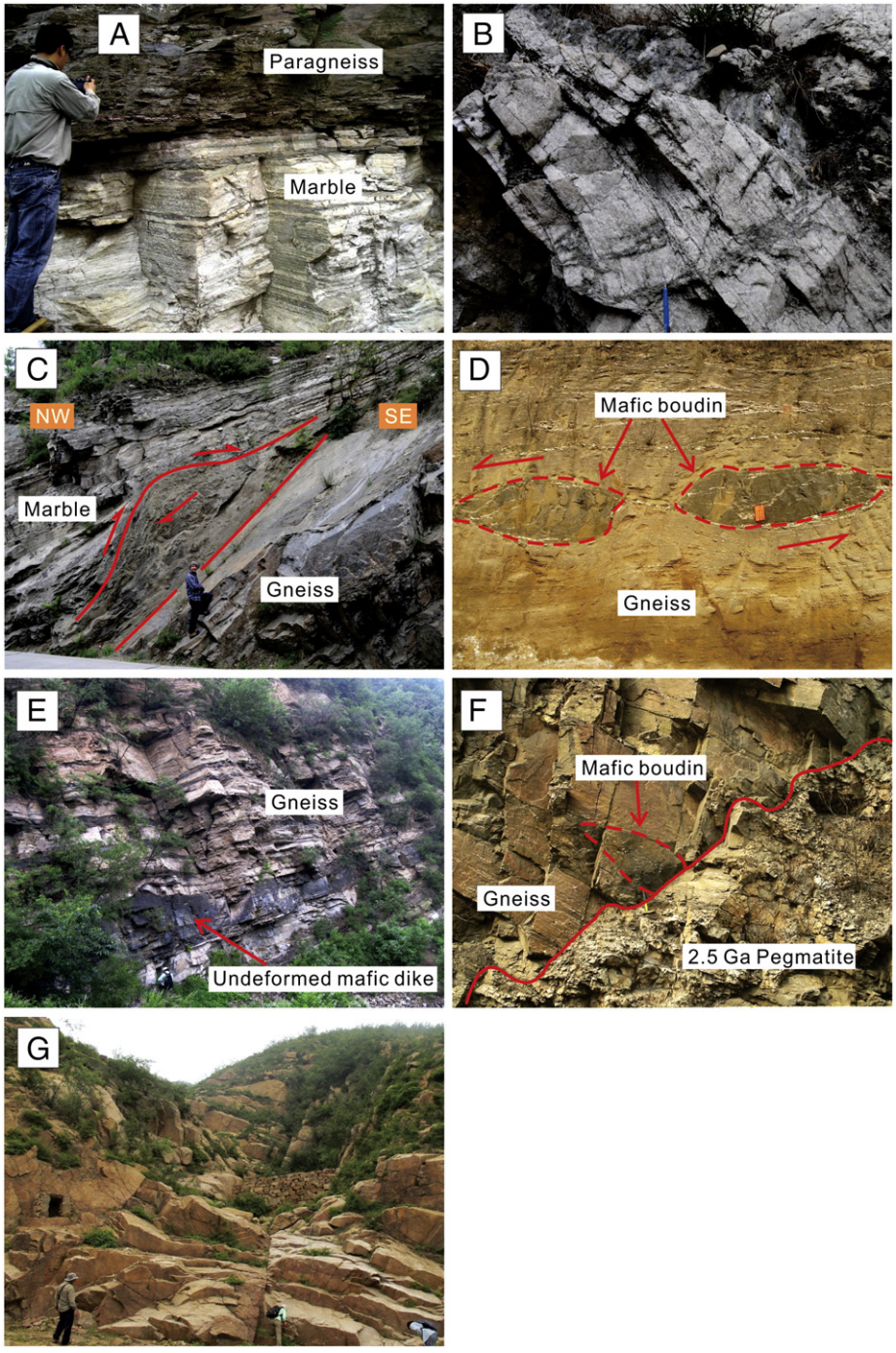

Fig. 5. Field photographs of the study area showing field relationships and lithological characteristics of different units in the study area. A: Tectonic contact between layered marble and paragneisses, north of Beixiaozhuang (N37°15′01″/E114°10′51″). B: Coarse grained marble layer of the marble unit, near Lujiazhuang (N37°13′16″/E114°6′16″). C: Marble layer thrust to southeast upon the TTG gneisses of the Eastern Zanhuang Domain forming the duplex structure, near Lujiazhuang (N37°13′06″/E114°6′05″). D: Amphibolite boudins preserved in the TTG gneisses of the Eastern Zanhuang Domain, near Lujiazhuang (N37°12′35″/E114°5′52″). E: Undeformed mafic dikes cross-cut the gneiss, west of Jiaozhuang (N37°16′39″/E114°8′02″). F: Late pegmatite cross-cutting the mafic boudins and TTG gneisses of Eastern Zanhuang Domain, near Lujiazhuang (N37°13′06″/E114°6′05″). G: Late granite (circa 2.5 Ga), near Wangjiazhuang (N37°18′02″/E114°13′30″).

of the TTG gneiss of the Eastern Zanhuang Domain, whereas the other belt demarcates the western-most series of the marble-siliciclastic unit (Figs. 2B and 3). The marble unit has structural contacts with the TTG gneisses of the Western Zanhuang Domain, the TTG gneisses of the Eastern Zanhuang Domain (Fig. 4), and the micaschist and paragneiss unit (Fig. 5A). The lower part of this unit is mainly composed of coarse-grained, foliated marble (Fig. 5B) up to 1 km thick, with structurally intercalated calc-silicate rocks, garnet amphibolitic dikes and fine-grained quartzite. The upper part is mainly composed of muscovite–biotite schist and banded quartzite. Micaschist, amphibolite, and marble are structurally repeated in some areas. The marble layer is in many places thrust upon the TTG gneisses of the Eastern Zanhuang Domian (Fig. 4) forming duplex structures near Lujiazhuang village (Figs. 5C and 2B for location).

Most of the marble is gray and white in color, with a small amount exhibiting pink and pale red colors. Both calc-silicate including calcite (45–55%) and wollastonite (50–60%) (Fig. 6A) and biotite–hornblende marble including calcite (70–75%), biotite (15–20%) and hornblende (10–15%) (Fig. 6B) are identified petrographically from this unit. The calc-silicate is mainly distributed in the northern part of the eastern-most marble belt of the marble-siliciclastic unit. The wollastonite is spatially associated with the pluton, and probably grew during contact metamorphism.

3.3.2. Micaschist and paragneiss unit

The micaschist and paragneiss unit structurally overlies the marble unit forming the core of a large synformal structure, with the marble unit outlining the boundaries of the synform, and bounded by thrust faults on its west and east margins (Figs. 2B and 3). It is composed of medium- to coarse-grained biotite-two feldspar schist, garnet schist, and garnet micaschist (Fig. 6C). The main minerals of the garnet-mica schist include garnet (35–40%), feldspar (15–20%), quartz (10–15%), muscovite (5–10%) and biotite (10–15%). This synform plunges gently north, resulting in the outcrop width of the micaschist and paragneiss unit decreasing from northeast to southwest (Figs. 2B and 3). The schist and gneiss of this unit are metamorphosed from a sedimentary protolith, with original rock types being greywacke, sandstone, and shale, akin to a flysch sequence.

3.4. Tectonic mélange unit

The mélange unit, which we informally name the Zanhuang mélange, crops out along the western margin of the marble-siliciclastic unit in thrust contact with the marble-siliciclastic unit and the TTG gneisses of the Western Zanhuang Domain (Figs. 2B and 3). It consists of a diverse suite of rocks including metapelites, metapsammites, marble, quartzite

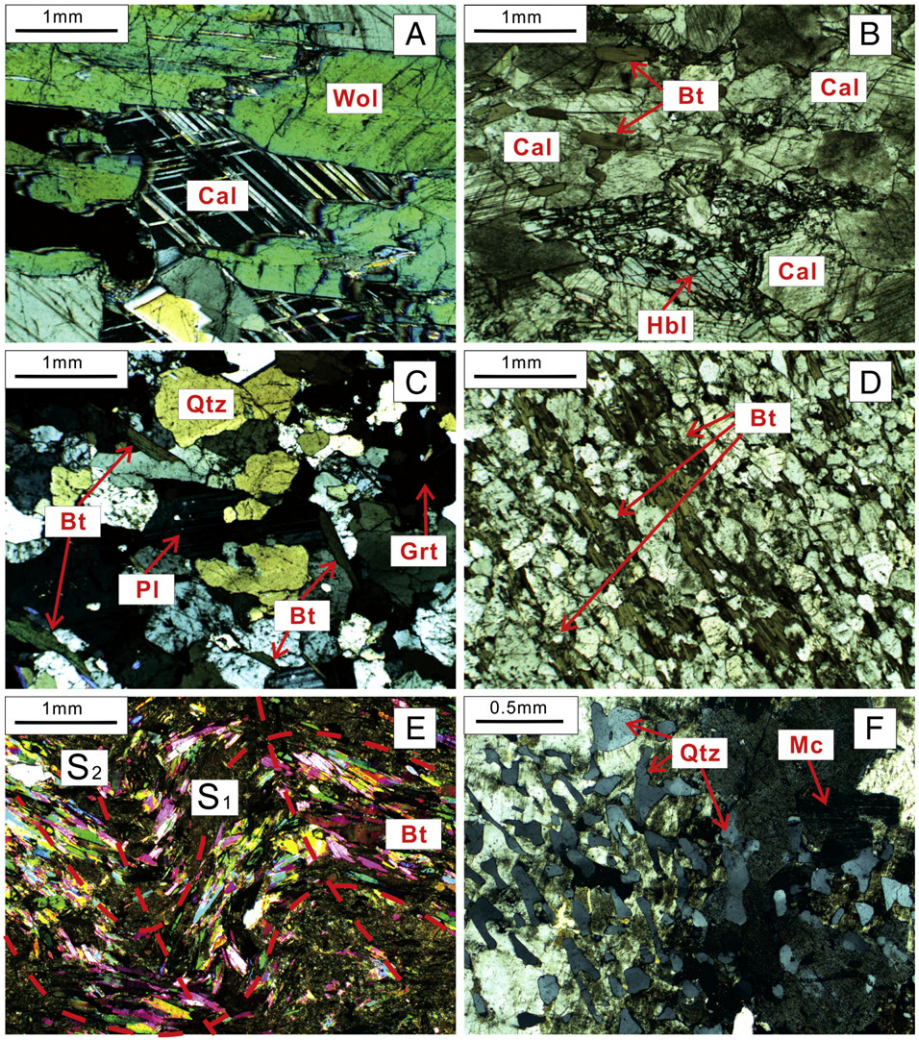

Fig. 6. Photomicrographs of different rock types and fabrics of different units in the study area. A: Calc-silicate with wollastonite (Wol) and calcite (Cal) (cross-polarized light). B: Marble with biotite (Bt) and hornblende (Hbl) (plane-polarized light). C: Schist with garnet (Grt), muscovite (Mus) and plagioclase (Pl) (cross-polarized light). D: Quartzofeldspathic mica gneiss with elongated biotite lineation (plane-polarized light). E: Biotite in micaschist outlining crenulation cleavage showing two stages of deformation (cross-polarized light). F: Pegmatite containing quartz (Qtz) and microcline (Mc) with graphic texture (cross-polarized light). All the photomicrographs are taken from probe thin sections (0.04 mm).

and exotic blocks of ultramafic and metagabbroic rocks, metabasalts that locally include relict pillow structures, and TTG gneisses.

The Zanhuang mélange includes many exotic mafic volcanic and ultramafic blocks, as well as carbonate rocks in a metapelitic to metapsammitic matrix (Fig. 7). The mafic volcanic and ultramafic blocks ranging from several tens of centimeters to several hundreds of meters in size, are concentrated in the northeastern part of the mapped area near Haozhuang village (Fig. 8), and all units in the mélange are intruded by a late granitic pluton. The relict pillow basalts with epidosite lenses in the cores of the deformed pillows are dispersed in amphibolite and metapelite matrices (Figs. 7A–B and 8), and have a structural contact with the paragneisses to the northwest (Fig. 8). Well-preserved epidosite outcrops are located northeast of Haozhuang village and south of Wangjiazhuang village in the northern part of the mélange (Fig. 2B). Fig. 7C shows the strongly deformed mélange complex with the blocks of rocks doleritic and relict pillows with epidosite cores in the highly sheared and folded metapelite matrix. Metagabbroic and ultramafic blocks are dispersed in the strongly deformed metapelite matrix (Fig. 7D–E). The petrographic and geochemical characteristics of these exotic mafic volcanic and ultramafic blocks have been described in Deng et al. (2013). In addition, marble blocks are dispersed in strongly deformed scaly micaschist interlayered with the discontinuous lenses of marble and scaly micaschist (Fig. 7F). Minor weakly metamorphosed fine- to medium-grained muscovite metasandstone and phyllite crop out east of Songjiazhuang village. Quartzite blocks are mainly distributed in gneisses in the northern part of the mélange.

Quartzofeldspathic mica gneiss containing an elongated biotite lineation (Fig. 6D) and biotite–quartz schist are mainly located in the central and southern part of the mélange unit. The biotite in the schist preserves good crenulation cleavage showing two stages of deformation (Fig. 6E). The main minerals of the quartzofeldspathic mica gneiss include quartz (20–30%), feldspar (40–50%), biotite (15–20%), staurolite (7–10%), garnet (3–5%) and minor opaque minerals.

3.5. Mafic dikes

Mafic dikes intrude all units of the study area including the TTG gneisses of the Western Zanhuang Domain in the COB, the TTG gneisses of the Eastern Zanhuang Domain in the Eastern Block, the marble-siliciclastic unit and the mélange of the Central Zanhuang Domain. The mafic dikes have experienced subsequent high pressure amphibolite facies (or higher) metamorphism and deformation and are highly sheared

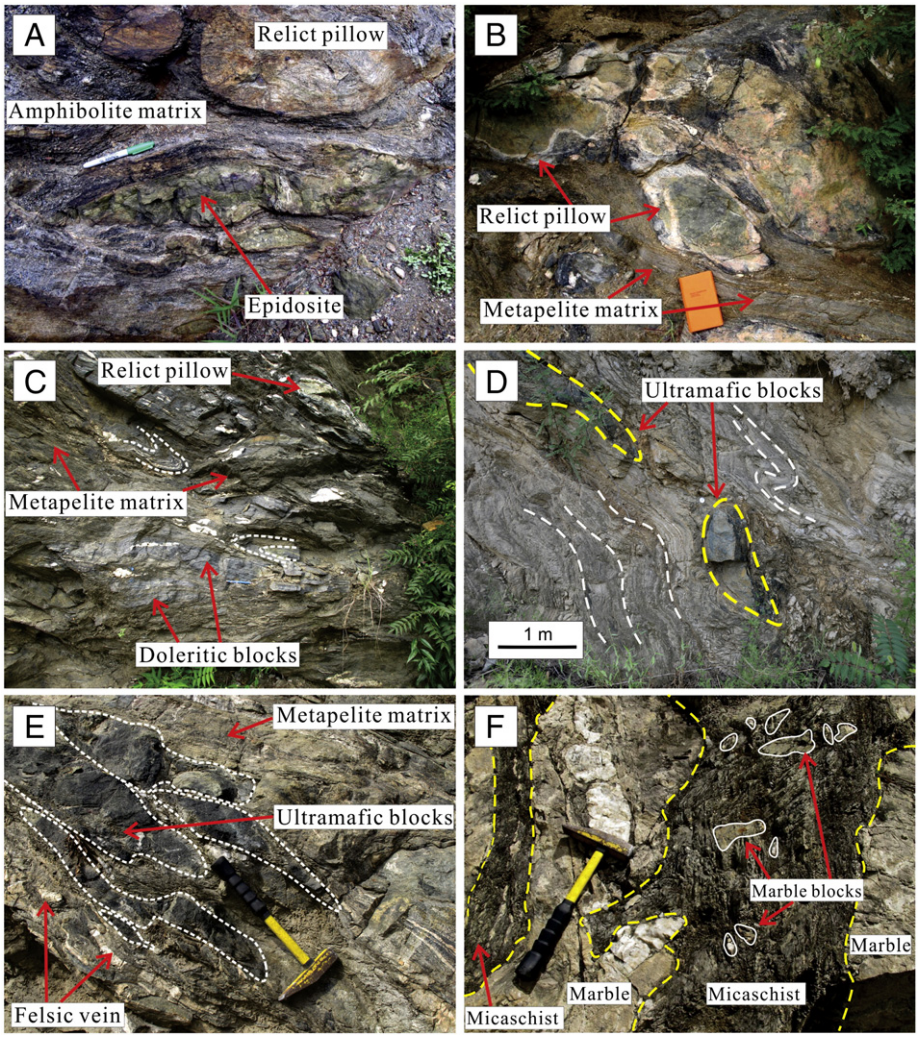

Fig. 7. Field photographs of various exotic blocks in different matrices. A: Deformed pillow structures with epidosite lenses preserved in the altered cores within the amphibolite matrix, northeast of Haozhuang village (N37°19′49″/E114°11′14″). B: Relict pillow dispersed in metapelite matrix, south of Wangjiazhuang village (N37°17′17″/E114°13′15″). C: Strongly sheared and deformed mélange complex with doleritic blocks and relict pillows with epidosite cores in the metapelite matrix structure, northeast of Haozhuang village (N37°19′42″/E114°11′02″). D: Ultramafic blocks in strongly deformed metapelite matrix, south of Haozhuang village (N37°18′40″/E114°9′46″). E: Ultramafic blocks dispersed in the metapelite matrix, north of Jiaozhuang village (N37°18′08″/E114°09′36″). F: Marble layer in strongly deformed micaschist forming the repetition between the layers of marble and scaly micaschist, small marble blocks dispersed in the strongly deformed micaschist, near Haozhuang village (N37°19′03″/E114°10′10″).

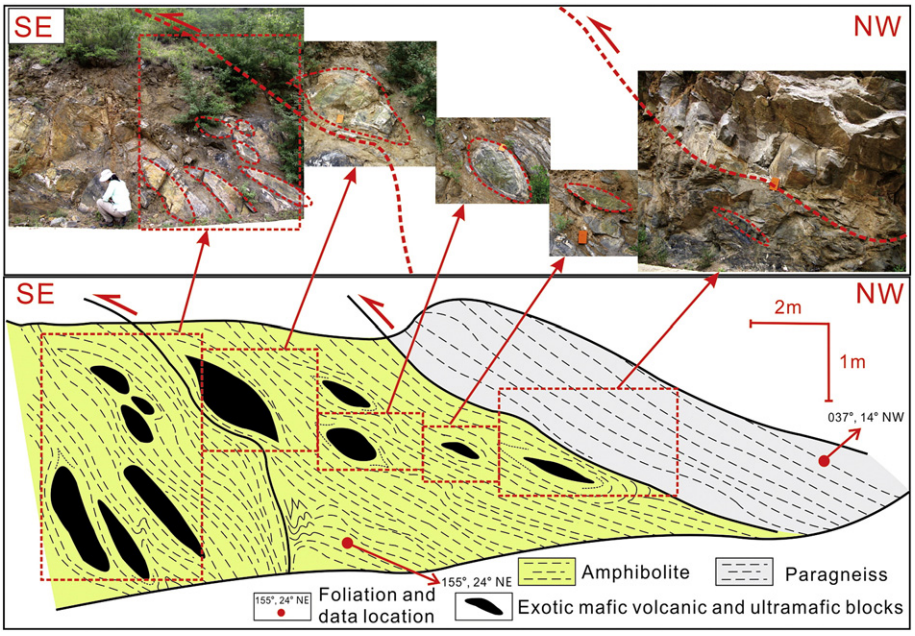

Fig. 8. Simplified sketch of exotic tectonic blocks of mafic volcanic and ultramafic rocks dispersed in amphibolite matrix, and the paragneiss thrusts towards the SE upon the amphibolite. Outcrop shown in Fig. 2B, near Wangjiazhuang village (N37°17′17″/E114°13′15″). The data show the strike and dip angle of the foliation.

and boudinaged, preserved now as amphibolitic boudins (Fig. 5D) that are derived from a mafic protolith (Deng et al., 2013). HBGMR (1996) suggested that the protoliths were possibly gabbro or diabase. The mafic boudins have different sizes ranging from a few meters to several hundred meters in length and a few meters to tens of meters in width. However, some original undeformed mafic dikes are still preserved in the relatively low strain areas (Fig. 5E), which is direct evidence that the boudins were derived from mafic dikes (Deng et al., 2013). In addition, the mafic boudins are cut by late 2.5 Ga pegmatites (Fig. 5F, see Section 6 for detailed geochronology analysis), indicating the ages of these mafic dikes are prior to 2.5 Ga. Most of the mafic dikes strike NE, dip to the NW with a moderate dip angle, and are mainly parallel to the gneissosity with poor continuity. The petrographic and geochemical characteristics of these mafic dikes have been described in Deng et al. (2013), who proposed that the highly sheared and boudinaged mafic dikes were generated from an arc-related mantle source.

3.6. Late granitic pluton and pegmatite

A late stage irregular ovoid-shaped monzogranite (Fig. 5G), which we informally name the Wangjiazhuang granite, intrudes the Zanhuang mélange unit (Figs. 2B and 3). Most of the foliations in the mélange strike NE and dip steeply NW (Fig. 2B, H–I), but the strike of the foliation is rotated into near-parallelism with the pluton margins. However, in some locations the late Wangjiazhuang granite truncates the early foliation in the mélange. There is a weak foliation in the pluton defined by the preferred orientation of feldspar grains, and in some locations near the margins of the pluton by the elongation of quartz ribbons. We interpret this to represent an emplacement-related magmatic foliation (e.g., Paterson and Tobisch, 1988; Paterson and Vernon, 1995; Vernon et al., 1989) that mimics the shape of the pluton margins, but is discordant with the earlier NE-striking foliation in the mélange at the NE and SW margins of the pluton, and parallel with the older foliation along the NW and SE pluton margins (Fig. 2B). The Wangjiazhuang granite is pale red with weakly gneissic and massive structure. The main minerals include feldspar (60–65%), quartz (30–35%), biotite (5–10%), muscovite (1–2%) and minor magnetite and apatite. Feldspar grains are mostly microcline and variably sericitized. There are minor marble, quartzite, and amphibolite inclusions distributed within the granite, ranging from several tens of centimeters to several meters in size (HBGMR, 1996).

Furthermore, pale red pegmatites that we relate to the granitic pluton cut many sections of the mélange, including the mafic boudins (Fig. 5F), the scattered marble unit and the gneisses of the Eastern Block (Figs. 2B and 3). These vary in size from several meters to several hundred meters in length and from several tens of centimeters to several meters in width. The undeformed pegmatites cross-cut the foliated gneisses of the Eastern Block with clear intrusive contact relationships showing that the pegmatites post-date the foliation in the mélange and other units (Fig. 9A–B). In some cases joints within the pegmatites are subparallel to the foliation of the gneiss, but these are clearly extensional joints and not related to the strong foliation in the surrounding mélange and other units (Fig. 9C–D). The pegmatites also cross-cut the scattered marble layer in the gneisses of Eastern Block (Fig. 9E-F). The marble layer dips shallowly to the SW. Late joints cross-cut the marble layer and the pegmatite (Fig. 9E-F). The pegmatite is undeformed and exhibits a graphic texture (Fig. 6F) as well as massive structure. The main minerals include microcline (50–55%), plagioclase (5–10%), quartz (15–20%), tourmaline (10–15%) and minor biotite and muscovite. Garnet-bearing pegmatites are also present in the study area.

4. Description of mélange fabrics and kinematics

The Zanhuang mélange consists of a structurally complex mixture of schists, gneisses and metasediments, with blocks and tectonic lenses of metabasalts, gabbros and ultramafic rocks (Fig. 10A). All rocks from the Zanhuang mélange are metamorphosed to amphibolite facies. Contacts between different units are structural, and individual units (blocks) can typically only be traced along strike for tens to hundreds of meters. Shear zones in the mélange matrix and along contacts between matrix and different blocks are characterized by asymmetric structures, composite planar fabrics, and scaly anastomosing foliations. The mélange unit is in thrust contact with the marble-siliciclastic unit to the southeast and the TTG gneisses from the Western Zanhuang Domain to the northwest, and shows strong deformation, shearing, and structural repetition of different units.

Analyses of asymmetric fabrics in mélanges have been well used to determine local and regional kinematics in many cases, such as the

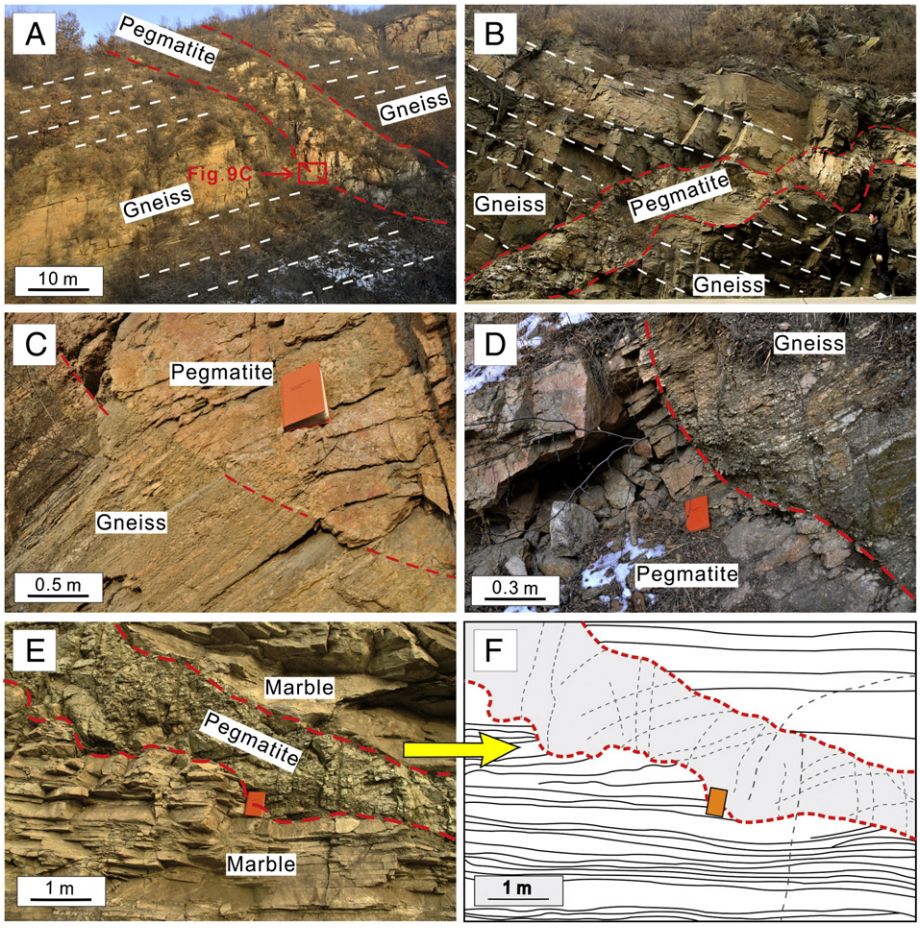

Fig. 9. Field photographs of pegmatite cross-cutting early fabrics. A and B: Undeformed circa 2.5 Ga pegmatite cross-cutting the foliation of the TTG gneisses in the Eastern Block, panel A (N37°13′29″/E114°06′23″) and panel B (N37°13′06″/E114°6′05″) near Lujiazhuang village. The white dashed lines in panels A–B represent the foliations in the gneiss. C and D: Pegmatite cross-cutting the foliation of the gneisses with late joint subparallel to the foliation. Location of panel C shown in panel A, panel D nearby panel A. E: Pegmatite cross-cutting marble layer, near Baihuzhuang village (N37°10′29″/E114°4′46″). F: Sketch of panel E. The black dashed lines in panel F represent the joints. The red dashed lines represent the contacts between the pegmatite and the country rocks.

Lopez Structural Complex in the San Juan Islands, the Franciscan mélange complex, the tectonic mélange along the Zagros Suture Zone, the Miyama Assemblage in the Shimanto Belt of southwest Japan and the McHugh mélange complex in the Kenai Peninsula of Alaska (e.g., Cowan and Brandon, 1994; Faghih et al., 2012; Festa et al., 2012; Fisher and Byrne, 1987; Hashimoto and Kimura, 1999; Kano et al., 1991; Kimura and Mukai, 1989; Kusky and Bradley, 1999; Needham, 1987; Needham and Mackenzie, 1988; Onishi and Kimura, 1995; Singleton and Cloos, 2012; Taira et al., 1988; Ujiie, 2002; Waldron et al., 1988). Indications of the sense of shear can be obtained from asymmetric features (Kano et al., 1991; Kusky and Bradley, 1999; Polat and Casey, 1995), which are abundant in the Zanhuang mélange. This section describes the different common fabrics found in the Zanhuang mélange and assesses the kinematic information.

Folds are widespread in most locations and rock types in the Zanhuang tectonic mélange unit (Fig. 10B–F), with rare sheath folds preserved in the chert fragments within the micaschist (Fig. 10B). The appearance of this folding indicates that the rocks experienced strong ductile deformation (e.g., Kusky and Bradley, 1999). Folds are also well preserved in the metapelites (Figs. 7C and 10C). In some cases, highly sheared felsic veins are folded with the foliation of the gneisses. Different sizes of folds are recognized within the gneisses in the mélange, ranging from several centimeters (Fig. 10D) to several tens of centimeters (Fig. 10E). In addition, angular folds within micaceous quartzite are also preserved in the northern part of the mélange near Haozhuang village (Figs. 2B and 10F). Fig. 11 shows that the paragneiss and amphibolites are strongly sheared and foliated. These asymmetric folds are commonly preserved in high shear strain layers, and can be used to obtain the overall sense of shear (Cowan and Brandon, 1994; Kusky and Bradley, 1999). The sense of shear across these high strain zones is described in Section 5 below.

Asymmetric extensional structures are abundant in the Zanhuang mélange. In some cases, scaly foliation, asymmetric tails around blocks or the shapes of blocks suggest a southeast-directed thrust sense of motion. A scaly foliation subparallel to the original lithological layering is preserved in the metasediments (Fig. 12A), and gives rise to the extension parallel to strike. Although experiencing high shear strains, the small blocks of mafic rocks within the micaschist (Fig. 12B) and the asymmetric tails around micaschist blocks (Fig. 12C) show obvious shear sense indicating thrusting to the southeast. The repetition of metasedimentary layers also shows evidence for the same sense of shearing forming the duplex structures (Fig. 12D).

Most kinematic indicators from the Zanhuang mélange show oblique slip with the hanging wall moving up to the southeast with respect to the footwall (marble-siliciclastic unit), consistent with an accretionary wedge setting (Fig. 3).

5. Structural analysis

A foliation marked by the gneissic layering of quartz and feldspar is developed within the TTG gneisses of the Western Zanhuang Domain

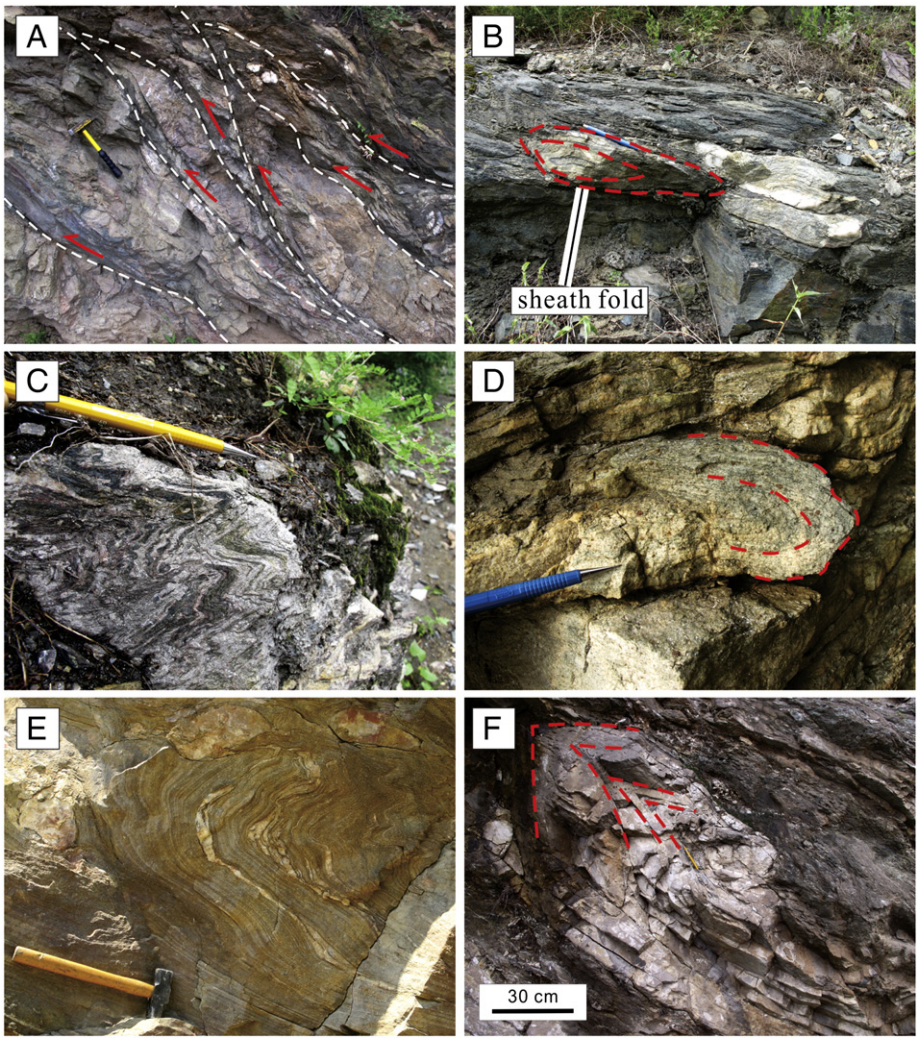

Fig. 10. Field photographs of thrusts and folds in different rock types of the Zanhuang mélange. A: Structural mélange fabrics composed of complex mixture of schists, gneisses and metasediments with thrusts, south of Haozhuang village (N37°17′59″/E114°9′35″). The white dashed lines show the thrust planes. B: Sheath fold of chert in the micaschist. The red dashed lines show the concentric structure on the plane which is perpendicular to the long axis (X axis) of the fold, south of Haozhuang village (N37°18′23″/E114°9′36″). C: Fold preserved in the metapelite, near Haozhuang village (N37°19′16″/E114°10′20″). D and E: Different scale of folds preserved in the gneisses, panel D located north of Shicao village (N37°16′59″/E114°9′25″), panel E located south of Wangjiazhuang village (N37°17′18″/E114°13′16″). F: Angular folded micaceous quartzite, northeast of Haozhuang village (N37°19′53″/E114°11′27″).

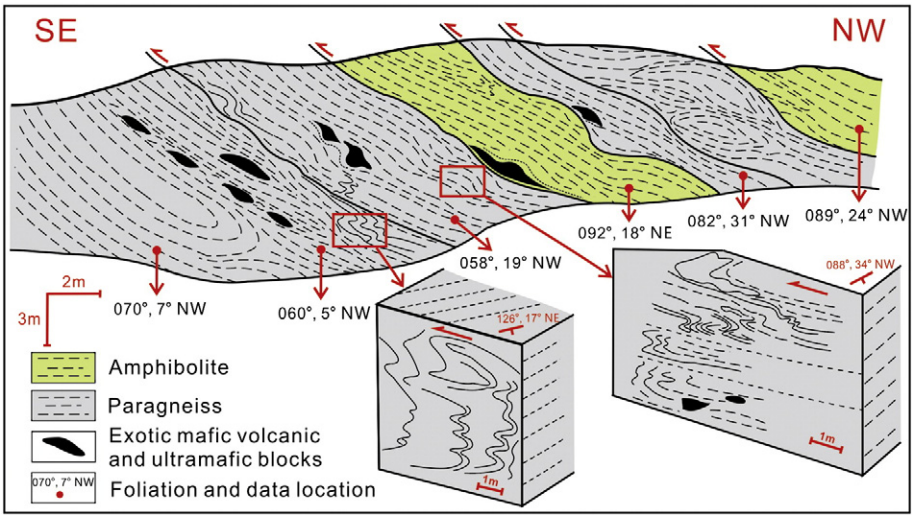

Fig. 11. Simplified sketch of southeast-directed thrust in the Zanhuang mélange between the interlayered paragneiss and amphibolite. Note that the exotic tectonic blocks of mafic volcanic and ultramafic rocks dispersed in the strongly foliated and folded paragneiss and amphibolite matrices. Outcrop shown in Fig. 2B, south of Haozhuang village (N37°18′27″/E114°09′35″). The data show the strike and dip angle of the foliation.

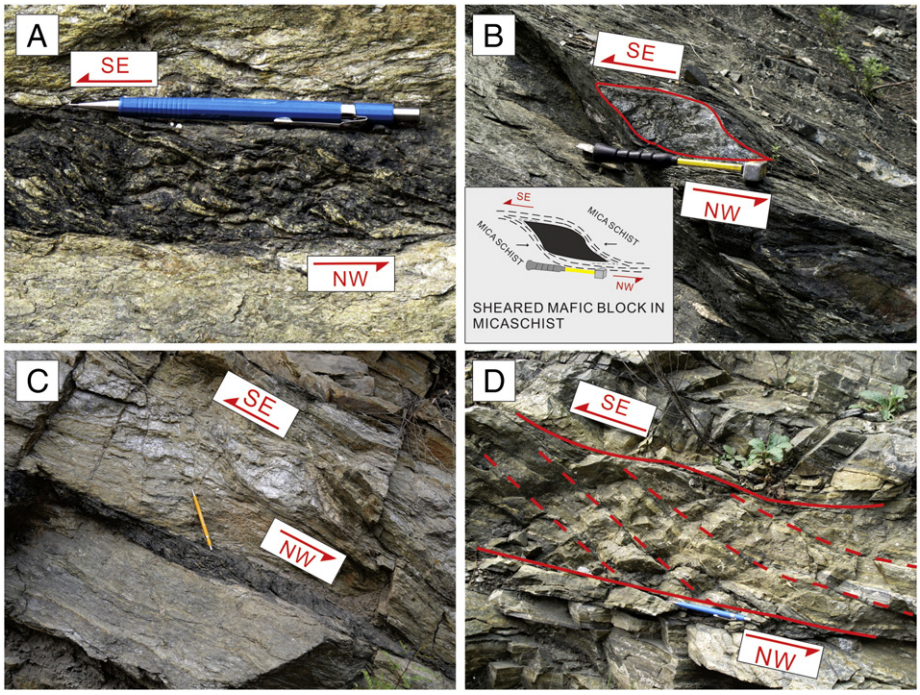

Fig. 12. Field photographs of asymmetric mélange fabrics. A: Scaly foliation in the metasediments show the southeast thrust, near Shicao village (N37°16′56″/E114°9′27″). B: Small blocks of mafic rock in the micaschist show the southeast thrust, south of Haozhuang village (N37°18′23″/E114°9′35″). C: Asymmetric tails around micaschist blocks show the southeast shearing, north of Shicao village (N37°16′55″/E114°9′27″). D: Repetition of metasediment layers in a duplex structure shows the southeast shear sense, north of Shicao village (N37°16′32″/E114°9′10″).

along the sheared contact zone with the Zanhuang mélange. The foliation dips shallowly (<40°) to the NW (Fig. 2C). A lineation defined by the preferred orientation of elongated mica is poorly preserved. This foliation in the Western Zanhuang Domain along the contact with the mélange developed due to the thrusting and deformation during the accretion process of the Zanhuang mélange.

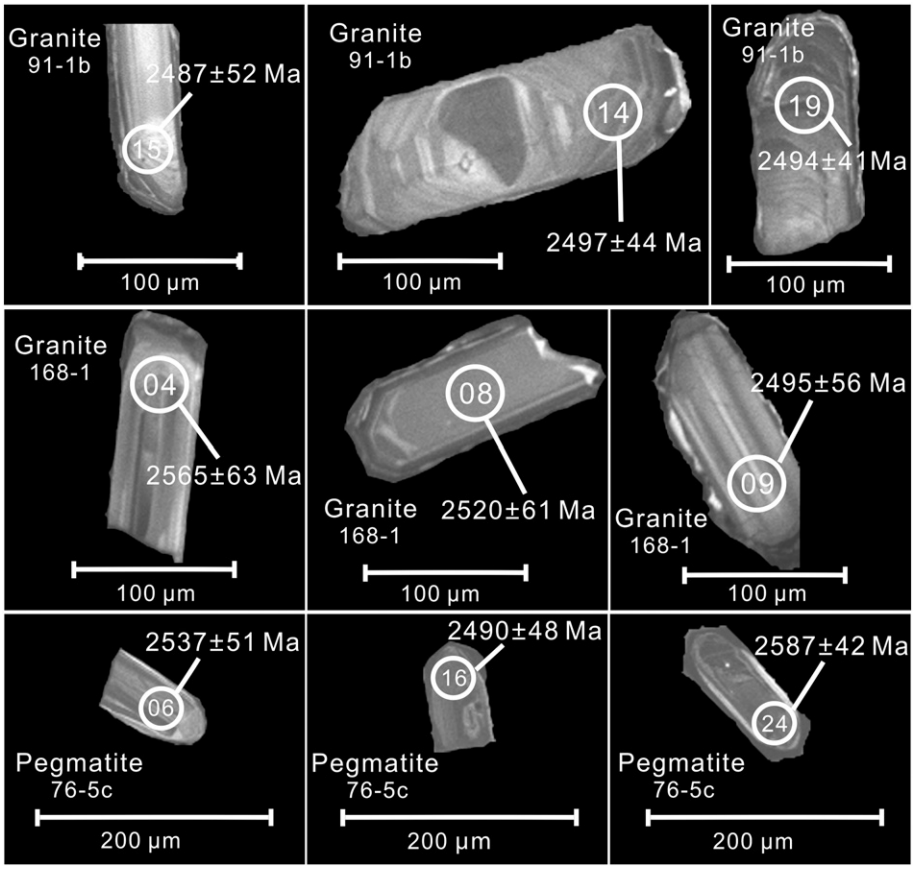

Fig. 13. Cathodoluminescence (CL) images of representative zircons from the two granite samples (91-1b and 168-1) and one cross-cutting pegmatite sample (76-5c).

A foliation is widely developed within the TTG gneisses of the Eastern Zanhuang Domain along the contact zone with the marble unit of the marble–siliciclastic sequence. The foliation marked by the gneissic layering of quartz and feldspar dips to the N in the northern part of Eastern Zanhuang Domain and to the NW in the southwestern part of Eastern Zanhuang Domain (Fig. 2B–D). The foliation surface contains a lineation plunging at 5–45° towards the NW (Fig. 2E).

A foliation occurs in the marble unit and micaschist and paragneiss of the carbonate/clastic sequence deposited on the western edge of the Eastern Block. The foliation dips shallowly (<35°) to the NW (Fig. 2F) in the southwestern part and dips N to NNE in the northern part of the marble–siliciclastic unit due to the intrusion of the Wangjiazhuang granite. A lineation is marked by the preferred orientation of biotite in the foliated marble and paragneiss. The data show that the lineation plunges at 5–25° towards the NW (Fig. 2G).

A foliation is widely developed within the tectonic mélange. The foliation is marked by the gneissic layering in the quartzofeldspathic gneisses and by a scaly schistosity of muscovite in the schist in the metapelitic units. The foliation throughout the mélange dips overall to NW, except that surrounding the late pluton, where it is deflected into a general concentric pattern surrounding the pluton (Fig. 2B, H–I). The foliation contains a lineation that is less developed and marked by the preferred orientation of elongated biotite and muscovite in the foliated gneiss and micaschist. Most of the data show that the lineation plunges towards the NW (Fig. 2J). Folds are abundant within most of the rock types in the mélange. Fig. 2K shows that the axial planes dip to the NW in the mélange and the fold hinges plunge at 10–50° towards the NW.

The structural elements described above show consistent trends with the regional structure that the TTG gneisses of Western Zanhuang Domain are thrust to the southeast upon the mélange units, and the highly sheared and deformed mélange unit with late mafic intrusions is thrust to the southeast upon the marble–siliciclastic unit.

6. Age of the Zanhuang mélange

Field observations demonstrate that the Zanhuang mélange is intruded by a granitic pluton and cross-cut by undeformed pegmatites. Two granite samples (91-1b and 168-1) and one pegmatite sample (76-5c) that cross-cut the structural fabrics in the mélange were selected for zircon U–Pb dating (sample locations shown in Fig. 2B). Laser ablation–inductively coupled plasma–mass spectrometry (LA–ICP–MS) was applied for the zircon U–Pb dating of the three samples at the State Key Laboratory of Geological Processes and Mineral Resources, China University of Geosciences (Wuhan). The operating conditions for the laser ablation system and the ICP-MS instrument, and data reduction procedures are the same as described by Liu et al. (2009, 2010). Off-line selection and integration of background and analysis signals, and time–drift correction and quantitative calibration for U–Pb dating were performed by ICPMSDataCal (Liu et al., 2009, 2010). Isoplot/Ex_version3 was used for making the concordia diagrams and weighted mean calculations (Ludwig, 2003). Cathodoluminescence (CL) images of representative zircons with well-developed zoning structures are shown as Fig. 13. Concordia plots of zircon dating results for granite and pegmatite are shown in Fig. 14. Data from these analyses are shown in Table 1. Zircon grains from the two granite samples have weighted mean $^{207}Pb/^{206}Pb$ ages of 2493 ± 22 Ma (91-1b) and 2540 ± 23 Ma (168-1), respectively. The pegmatite yields weighted mean $^{207}Pb/^{206}Pb$ age of 2539 ± 44 Ma (76-5c). All three samples demonstrate an age of circa 2500 Ma for these late magmatic rocks that cross-cut the structural fabrics in the Zanhuang mélange.

7. Conclusions and tectonic implications

We have documented an Archean mélange that consists of a mixture of metapelitic, metapsammitic, marble, mafic and ultramafic rocks, and

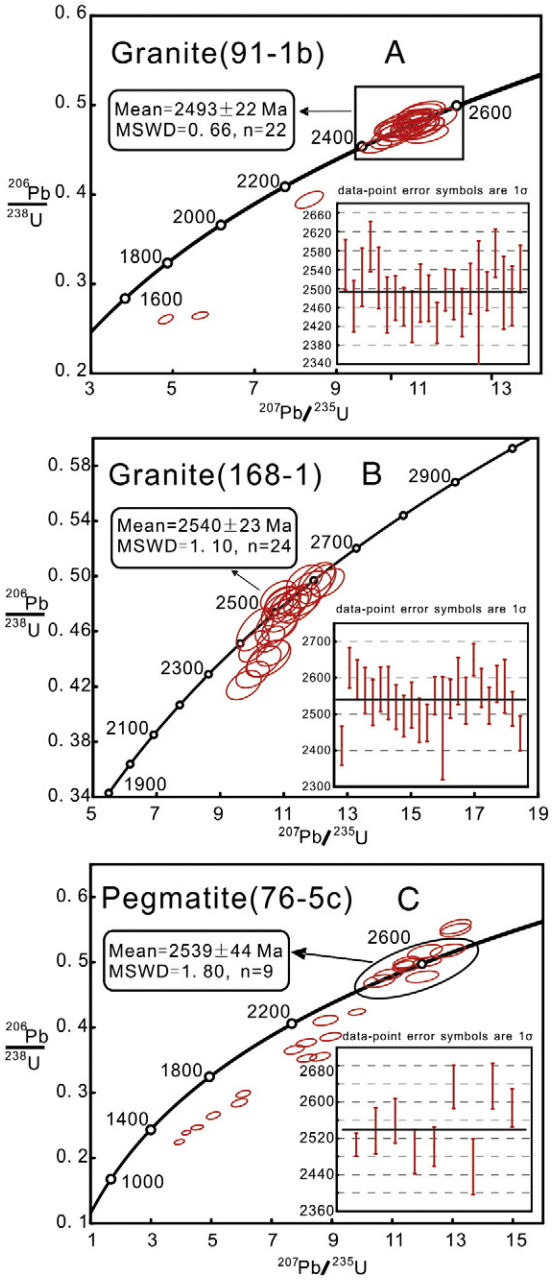

Fig. 14. Concordia plots show the zircon dating results of granite (91-1b(A) and 168-1(B)) and pegmatite (76-5c(C)) of the study area in Zanhuang Massif. MSWD-mean square of weighted deviates. See Fig. 2B and Table 1 for sample locations and details of analyses.

TTG gneisses in the Zanhuang Massif of the NCC. The mélange marks the tectonic boundary between two different tectonic blocks (Western Zanhuang Domain in the COB and Eastern Block) in the NCC. The protolith of the TTG gneisses in the Western Zanhuang Domain is predominantly tonalite, and one sample has a SHRIMP zircon U–Pb age of circa 2692 ± 12 Ma, and represents the arc terrane correlated with the Fuping terrane (Trap et al., 2009a). However, the TTG gneisses of the Eastern Block have ages ranging from early to late Archean, and may have formed as an arc that collided to form a continental block, that was broken apart by rifting at circa 2.7 Ga, with subsequent deposition of a passive margin sequence on its western margin (Kusky, 2011a,b; Kusky and Li, 2003; Kusky et al., 2007a,b; Nutman et al., 2011). The passive margin on the western edge of the Eastern Block is strongly deformed, and imbricated with the basement gneisses, and overthrust by the generally younger TTG gneisses of the Western Zanhuang Domain. In between, the Zanhuang mélange marks the

Table 1
LA-ICP-MS zircon U–Pb data for the late granite (91-1b and 168-1) and cross-cutting pegmatite (76-5c) from the study area of Zanhuang Massif, North China Craton.

	Pb (ppm)	Th (ppm)	U (ppm)	Measured ratios								Calculated ages (Ma)							
				$^{207}Pb/^{206}Pb$	1 s	$^{207}Pb/^{235}U$	1 s	$^{206}Pb/^{238}U$	1 s	$^{208}Pb/^{232}Th$	1 s	$^{207}Pb/^{206}Pb$	1 s	$^{207}Pb/^{235}U$	1 s	$^{206}Pb/^{238}U$	1 s	$^{208}Pb/^{232}Th$	1 s
Sample 91-1b granite (N37°18′2.2″, E114°13′29.9″)																			
91-1b-1	5.519	9.67	9.35	0.1691	0.0059	11.1001	0.3510	0.4723	0.0084	0.1301	0.0051	2550	53	2532	29	2494	37	2473	92
91-1b-2	24.04	23.9	88.5	0.1606	0.0052	11.0949	0.3701	0.4904	0.0077	0.1562	0.0078	2463	54	2531	31	2572	33	2933	137
91-1b-3	7.761	10.1	13.4	0.1665	0.0056	10.9189	0.3391	0.4721	0.0080	0.1365	0.0054	2524	62	2516	29	2493	35	2586	96
91-1b-4	7.660	10.4	13.3	0.1721	0.0055	11.2034	0.3492	0.4656	0.0066	0.1325	0.0044	2589	53	2540	29	2464	29	2514	78
91-1b-5	12.41	20.2	20.8	0.1654	0.0063	10.9173	0.3950	0.4757	0.0080	0.1445	0.0052	2522	65	2516	34	2509	35	2728	92
91-1b-6	11.07	15.2	18.0	0.1609	0.0055	10.3958	0.3722	0.4640	0.0098	0.1335	0.0050	2466	59	2471	33	2457	43	2532	90
91-1b-7	10.24	14.9	17.4	0.1622	0.0046	10.9289	0.3118	0.4816	0.0070	0.1433	0.0047	2480	47	2517	27	2534	30	2706	82
91-1b-8	16.93	19.1	28.1	0.1606	0.0038	10.3660	0.2415	0.4609	0.0055	0.1334	0.0034	2461	40	2468	22	2443	24	2531	60
91-1b-9	90.03	74.9	169	0.1586	0.0050	10.4826	0.3259	0.4716	0.0066	0.1366	0.0045	2440	54	2478	29	2490	29	2588	81
91-1b-10	19.59	19.6	33.7	0.1633	0.0060	10.9408	0.3715	0.4815	0.0082	0.1290	0.0054	2490	61	2518	32	2534	36	2452	96
91-1b-11	12.83	12.6	21.2	0.1623	0.0048	10.8894	0.3254	0.4823	0.0071	0.1374	0.0047	2480	49	2514	28	2537	31	2602	84
91-1b-12	19.97	19.6	33.2	0.1574	0.0045	10.3836	0.2969	0.4747	0.0069	0.1221	0.0038	2427	43	2470	26	2504	30	2329	69
91-1b-13	22.82	27.8	37.9	0.164	0.0043	10.7708	0.2934	0.4716	0.0062	0.1283	0.0039	2497	44	2504	25	2491	27	2440	90
91-1b-14	31.40	30.1	53.2	0.1631	0.0051	11.0240	0.3584	0.4884	0.0074	0.1368	0.0053	2487	52	2525	30	2564	32	2591	94
91-1b-15	24.83	18.7	41.1	0.1594	0.0048	10.4119	0.3222	0.4721	0.0069	0.1336	0.0049	2450	51	2472	29	2493	30	2534	88
91-1b-16	37.85	31.8	65.7	0.1632	0.0051	10.5741	0.3524	0.4688	0.0073	0.1346	0.0050	2500	53	2486	31	2478	32	2552	90
91-1b-17	18.24	17.7	29.7	0.1589	0.0040	9.9646	0.2515	0.4523	0.0052	0.1406	0.0050	2444	−157	2432	23	2405	23	2659	88
91-1b-18	46.24	19.8	85.9	0.1637	0.0040	10.9113	0.2804	0.4807	0.0062	0.1341	0.0039	2494	41	2516	24	2530	27	2544	70
91-1b-19	83.14	56.5	138	0.1718	0.0053	11.4047	0.3530	0.4811	0.0087	0.1244	0.0051	2575	51	2557	29	2532	38	2370	92
91-1b-20	26.64	25.7	43.9	0.1634	0.0042	10.9369	0.2808	0.4813	0.0051	0.1852	0.0057	2491	77	2518	24	2533	22	3434	97
91-1b-21	282.8	137	463	0.1627	0.0062	10.7001	0.4264	0.4779	0.0102	0.1509	0.0076	2484	63	2497	37	2518	44	2841	33
91-1b-22	13.92	11.9	22.8	0.1648	0.0050	11.0117	0.3264	0.4736	0.0070	0.1337	0.0052	2542	49	2524	28	2499	30	2536	93
91-1b-23	63.61	27.3	142	0.1328	0.0032	4.8315	0.118	0.2585	0.0034	0.1165	0.0036	2135	41	1790	21	1482	18	2228	65
91-1b-24	26.77	24.5	43.2	0.1554	0.0038	8.3730	0.2263	0.3904	0.0063	0.1329	0.0059	2395	43	2272	25	2125	29	2522	105
91-1b-25	199	238	570	0.1551	0.0036	5.6697	0.1298	0.2628	0.0026	0.1060	0.0027	2403	39	1927	20	1504	13	2036	49
Sample 168-1 granite (N37°19′37.2″, E114°11′19.6″)																			
168-1-1	5.94	6.83	12.3	0.1560	0.0049	10.0963	0.3860	0.4612	0.0103	0.1582	0.0070	2413	54	2444	35	2445	45	2969	121
168-1-2	4.47	5.69	7.73	0.1772	0.0059	12.0611	0.3821	0.4942	0.0093	0.1444	0.0060	2628	56	2609	30	2589	40	2725	106
168-1-3	6.52	9.39	11.0	0.1738	0.0056	12.0336	0.3775	0.4979	0.0079	0.1457	0.0050	2595	54	2607	29	2605	34	2749	88
168-1-4	5.95	7.72	11.1	0.1706	0.0064	10.3639	0.3622	0.4381	0.0073	0.1376	0.0069	2565	63	2468	32	2342	33	2606	123
168-1-5	12.03	14.0	23.4	0.1675	0.0062	10.0238	0.3454	0.4286	0.0062	0.1287	0.0052	2532	63	2437	32	2299	28	2448	94
168-1-6	17.59	16.7	30.0	0.1710	0.0057	11.5767	0.3771	0.4809	0.0066	0.1402	0.0051	2569	61	2571	30	2531	29	2652	90
168-1-7	5.40	6.33	9.98	0.1701	0.0073	10.5287	0.4537	0.4401	0.0088	0.1415	0.0076	2558	73	2482	40	2351	39	2675	135
168-1-8	11.74	17.7	19.5	0.1662	0.0060	10.9540	0.3665	0.4717	0.0081	0.1335	0.0049	2520	61	2519	31	2491	35	2533	87
168-1-9	15.34	12.3	27.9	0.1637	0.0055	10.7965	0.3299	0.4756	0.0077	0.1377	0.0058	2495	56	2506	28	2508	34	2608	104
168-1-10	14.41	22.6	23.5	0.1667	0.0062	11.1583	0.4077	0.4786	0.0080	0.1435	0.0057	2525	63	2536	34	2521	35	2711	101
168-1-11	17.12	21.8	29.4	0.1625	0.0059	10.9574	0.3812	0.4804	0.0075	0.1410	0.0060	2483	61	2520	32	2529	33	2665	106
168-1-12	33.31	30.5	61.1	0.1618	0.0050	10.9558	0.3526	0.4828	0.0067	0.1468	0.0052	2476	52	2519	30	2539	29	2769	92
168-1-13	23.82	25.2	40.7	0.1693	0.0054	11.3391	0.3468	0.4819	0.0069	0.1371	0.0048	2551	52	2551	29	2536	30	2597	86
168-1-14	26.61	30.3	45.8	0.1604	0.0055	10.8313	0.3688	0.4854	0.0074	0.1281	0.0046	2461	−142	2509	32	2551	32	2436	82
168-1-15	58.51	37.2	104	0.1684	0.0054	11.6544	0.3746	0.4969	0.0074	0.1277	0.0046	2543	53	2577	30	2600	32	2429	83
168-1-16	20.65	19.0	34.4	0.1735	0.0067	11.7877	0.4614	0.4903	0.0088	0.1307	0.0057	2592	65	2588	37	2572	38	2484	101
168-1-17	18.62	30.0	32.7	0.1679	0.0064	9.7427	0.3608	0.4210	0.0069	0.1288	0.0047	2537	64	2411	34	2265	31	2449	84
168-1-18	44.78	39.4	71.5	0.1796	0.0047	12.3835	0.3421	0.4952	0.0068	0.1394	0.0044	2650	45	2634	26	2593	29	2637	77
168-1-19	9.750	10.2	15.8	0.1714	0.0060	11.4590	0.4403	0.4803	0.0094	0.1562	0.0081	2572	53	2561	36	2528	41	2934	141
168-1-20	26.65	24.2	45.0	0.1666	0.0050	10.8656	0.3643	0.4631	0.0068	0.1450	0.0052	2524	51	2512	31	2453	30	2736	91
168-1-21	21.41	19.2	36.7	0.1725	0.0051	10.6588	0.3366	0.4441	0.0062	0.1432	0.0057	2583	50	2494	29	2369	28	2705	100
168-1-22	12.61	14.1	20.4	0.1720	0.0076	10.8144	0.4695	0.4667	0.0111	0.1621	0.0087	2577	74	2507	40	2469	49	3036	152
168-1-23	38.13	37.9	63.7	0.1657	0.0041	10.5973	0.2848	0.4544	0.0062	0.1342	0.0047	2515	47	2488	25	2415	28	2545	84
168-1-24	30.63	26.3	54.2	0.1592	0.0044	10.0617	0.3116	0.4490	0.0075	0.1287	0.0049	2447	48	2440	29	2391	33	2448	88
Sample 76-5c pegmatite (N37°13′13.8″, E114°06′22.1″)																			
76-5c-1	40.58	51.9	73.0	0.1649	0.0025	11.3971	0.2106	0.4952	0.0045	0.1245	0.0021	2506	25	2556	17	2593	20	2372	38
76-5c-2	245.9	113	515	0.1656	0.0027	9.8329	0.1861	0.4238	0.0032	0.2464	0.0045	2513	26	2419	17	2277	14	4452	73
76-5c-3	101.1	112	403	0.1246	0.0026	4.1715	0.0961	0.2390	0.0023	0.0706	0.0018	2033	38	1668	19	1381	12	1380	34
76-5c-4	65.60	97.7	158	0.1653	0.0041	8.1691	0.2143	0.3530	0.0038	0.0971	0.0027	2511	43	2250	24	1949	18	1873	49
76-5c-5	85.10	112	263	0.1490	0.0042	5.9329	0.1756	0.2846	0.0041	0.1164	0.0034	2334	48	1966	26	1614	21	2225	62
76-5c-6	32.40	38.9	53.5	0.1679	0.0051	11.5271	0.3435	0.4956	0.0068	0.1338	0.0046	2537	51	2567	28	2595	30	2537	83
76-5c-7	161.4	62.5	264	0.1714	0.0042	13.1001	0.3348	0.5493	0.0065	0.2499	0.0070	2572	40	2687	24	2822	27	4509	113
76-5c-8	219.0	91.4	347	0.1700	0.0040	13.1010	0.3399	0.5545	0.0074	0.2812	0.0079	2558	39	2687	24	2844	31	5009	124
76-5c-9	119.2	129	429	0.1334	0.0040	4.5337	0.1342	0.2468	0.0025	0.0671	0.0025	2142	47	1737	25	1422	13	1313	47
76-5c-10	99.30	61.7	161	0.1701	0.0050	12.0848	0.3787	0.5158	0.0074	0.1693	0.0058	2558	49	2611	29	2681	31	3162	100
76-5c-11	95.00	182	194	0.1573	0.0042	8.1510	0.2211	0.3764	0.0041	0.0825	0.0024	2427	46	2248	25	2059	19	1602	45
76-5c-12	121.8	139	330	0.1480	0.0038	6.0618	0.1564	0.2981	0.0036	0.1109	0.0032	2324	43	1985	22	1682	18	2126	58
76-5c-13	146.4	132	463	0.1378	0.0036	5.0702	0.1505	0.2651	0.0037	0.0722	0.0025	2200	45	1831	25	1516	19	1409	47
76-5c-14	66.49	35.0	136	0.1546	0.0046	8.7892	0.2717	0.4108	0.0051	0.1344	0.0047	2398	51	2316	28	2219	23	2549	84
76-5c-15	95.70	85.6	157	0.1633	0.0047	10.8715	0.3169	0.4812	0.0057	0.1297	0.0039	2490	48	2512	27	2532	25	2465	71
76-5c-16	164.5	95.9	388	0.1516	0.0040	7.7539	0.2182	0.3660	0.0045	0.1072	0.0032	2365	46	2203	25	2011	21	2058	59
76-5c-17	73.50	59.0	117	0.1644	0.0042	11.4785	0.2949	0.5000	0.0058	0.1391	0.0040	2502	43	2563	24	2614	25	2633	72
76-5c-18	61.50	61.9	90.3	0.1767	0.0051	12.8409	0.3822	0.5175	0.0068	0.1523	0.0047	2633	48	2668	28	2689	29	2866	83
76-5c-19	64.10	58.2	112	0.1601	0.0053	10.5752	0.3423	0.4713	0.0065	0.1329	0.0044	2457	61	2487	30	2489	28	2522	78

Table 1 (*continued*)

	Pb (ppm)	Th (ppm)	U (ppm)	Measured ratios								Calculated ages (Ma)							
				$^{207}Pb/^{206}Pb$	1 s	$^{207}Pb/^{235}U$	1 s	$^{206}Pb/^{238}U$	1 s	$^{208}Pb/^{232}Th$	1 s	$^{207}Pb/^{206}Pb$	1 s	$^{207}Pb/^{235}U$	1 s	$^{206}Pb/^{238}U$	1 s	$^{208}Pb/^{232}Th$	1 s
76-5c-20	291.6	97.5	478	0.1779	0.0053	11.9942	0.3587	0.4778	0.0059	0.2796	0.0095	2635	50	2604	28	2518	26	4983	149
76-5c-21	217.4	158	834	0.1246	0.0034	3.9426	0.1105	0.2246	0.0026	0.0788	0.0024	2033	50	1622	23	1306	14	1533	45
76-5c-22	209.6	108	468	0.1723	0.0043	8.6067	0.2232	0.3551	0.0043	0.1798	0.0056	2580	41	2297	24	1959	20	3342	95
76-5c-23	197.8	193	300	0.1729	0.0043	12.1600	0.3082	0.5008	0.0048	0.1248	0.0034	2587	42	2617	24	2617	21	2377	61
76-5c-24	261.5	97.6	561	0.1693	0.0042	9.0456	0.2333	0.3817	0.0041	0.1707	0.0060	2551	42	2343	24	2084	19	3185	103

Zircons from the intrusive granite and cross-cutting pegmatite of the mélange unit were dated using LA–ICP-MS technique at the State Key Laboratory of Geological Processes and Mineral Resources, China University of Geosciences (Wuhan) following the analytical procedures of Liu et al. (2010b).

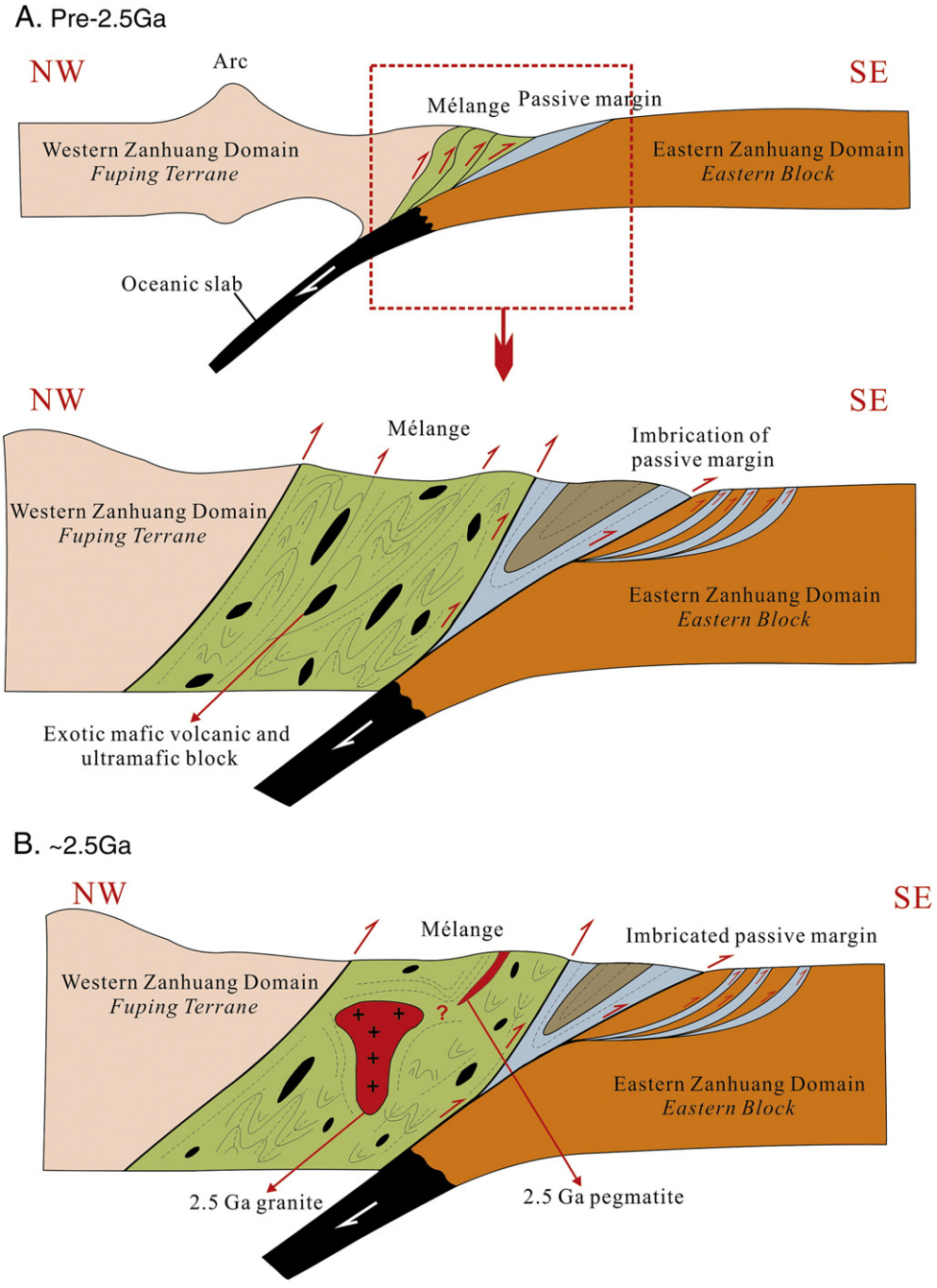

Fig. 15. Model for tectonic evolution of North China craton in the late Archean. Note that an arc (Western Zanhuang Domain) in the COB collided with the Eastern Block (Eastern Zanhuang Domain) prior to 2.5 Ga, leading to the formation of the Zanhuang mélange in between, and late granitic pluton and pegmatite intruded in the mélange at circa 2.5 Ga.

suture zone between the intra-oceanic arc or fore-arc terrane in the COB and Eastern Block continent (Fig. 15A). The sequence of rocks of marble–siliciclastic unit composed mainly of coarse-grained marble, fine-grained quartzite, intercalated calc-silicate rocks, muscovite–biotite schist, and late garnet amphibolitic dikes, is consistent with the rock types from passive margins to foreland basins. We interpret the marble–siliciclastic unit as a passive margin sequence to foreland basin sequence developed on the western margin of the Eastern Block (Fig. 15A). Kusky and Li (2003) first proposed that these sedimentary sequences deposited along the western edge of the Eastern Block represent a passive continental margin and foreland basin sequence. The Zanhuang mélange is intruded by a circa 2.5 Ga Wangjiazhuang granitic pluton, and cut by undeformed circa 2.5 Ga pegmatites, providing a minimum age for the arc–continent collision (Fig. 15B). We suggest that the granite and pegmatite were generated from the partial melting of the thickened crust due to the subsequent reversal of subduction polarity to east-dipping beneath the arc–continent collision zone after the arc was sutured to the Eastern Block continent (Deng et al., 2013), then both intruded into the mélange at circa 2.5 Ga. The analysis of field observations and structural fabrics shows that the Western Zanhuang Domain was thrust upon the Eastern Zanhuang Domain to the southeast due to the arc-continent collision between the arc terrane in the COB and the Eastern Block during intra-oceanic northwestward-directed subduction. We therefore demonstrate that the arc terrane in the COB (Fuping terrane) and the Eastern Block collided prior to 2.5 Ga, consistent with a late Archean suturing event of the western margin of the Eastern Block with an arc terrane during arc–continent collision.

Some Archean terranes have geological characteristics similar to Phanerozoic subduction–accretion complexes (Hoffman, 1991; Kusky, 1989; Kusky and Polat, 1999; Polat et al., 1998; Şengör and Natalin, 1996; Taira et al., 1992; Windley, 1993). There are only a few general descriptions of Archean mélanges (de Wit et al., 1992; Kusky, 1990; Kusky and Polat, 1999; Lin et al., 1996; Polat and Kerrich, 1999; Wang et al., 1996). The Archean Zanhuang mélange described here contains a mixture of structurally bounded blocks of metamorphosed pillow basalt, diabase, gabbro, and ultramafic rocks, in a highly sheared metapelitic and amphibolitic matrices, with numerous tectonic slices of psammites that resemble trench turbidites. This Archean mélange is remarkably similar to other accretionary mélanges in younger orogens that mark the sites of former plate subduction and convergence, separating a thick carbonate and clastic shelf-type sequence on one side, from a magmatic arc on the other side. The similarities to younger mélanges also include the range of matrix and exotic block rock types, the structural style, kinematics, and sequence of structural and magmatic events. Compared to Archean mélanges, Phanerozoic mélanges are characterized by lithologically more diverse blocks, including biogenic carbonates, radiolarian cherts, and other rocks related to changes in the Earth's biosphere, atmosphere, and geosphere (e.g., Kusky et al., 2013). In addition, blueschists and eclogites have not been convincingly documented in Archean terrains (Stern, 2007), but the previous claims that Archean subduction-related mélanges do not exist no longer hold water. The lack of blueschist and eclogite facies metamorphic rocks in Archean subduction–accretion terranes, is probably due to the elevated thermal gradients and shallow-angle subduction or overprinting during later collisional and tectonomagmatic events (Condie, 1997; Polat and Kerrich, 1999; Polat et al., 1998; Wakabayashi, 1996).

In this study, the clear association of rock types and structures in the 2–10 km wide Archean tectonic mélange in Zanhuang Massif, Central Orogenic Belt, North China Craton, cut by 2.5 Ga granite and undeformed 2.5 Ga pegmatite, suggests strongly that modern-style plate tectonics was operating by the end of the Archean.

Acknowledgments

This study was supported by the National Natural Science Foundation of China (No. 91014002) and the Ministry of Education of China (No. B07039). Ali Polat acknowledges funding from NSERC Discovery Grant 250926. We appreciate Maarten de Wit and an anonymous reviewer for comments that substantially improved the manuscript, and Mian liu for his helpful editorial comments. We thank Mingguo Zhai from the Institute of Geology and Geophysics, Chinese Academy of Sciences for Constructive discussion before the field work. We also thank Lingling Xiao from the Institute of Geology, Chinese Academy of Geological Sciences, and Zhensheng Wang, Jianmin Fu, and Traore Alhousseyni from China University of Geosciences (Wuhan) for helping with the field work.

References

Bai, J., Dai, F.Y., 1996. The early Precambrian crustal evolution of China. Journal of Southeast Asian Earth Sciences 13, 205–214.
Cawood, P.A., Kröner, A., Collins, W.J., Kusky, T.M., Mooney, W.D., Windley, B.F., 2009. Accretionary orogens through Earth history. Geological Society of London, Special Publication 318, 1–36.
Condie, K.C., 1997. Plate Tectonics and Crustal Evolution, fourth edition. Butterworth-Heinemann, Newton.
Cowan, D.S., Brandon, M.T., 1994. A symmetry-based method for kinematic analysis of large-slip brittle fault zones. American Journal of Science 294, 257–306.
de Wit, M.J., Jones, M.G., Buchanan, D.L., 1992. The geology and tectonic evolution of the Pietersburg greenstone belt, South Africa. Precambrian Research 55, 123–153.
Deng, H., Kusky, T.M., Polat, A., Wang, L., Wang, J.P., Wang, S.J., 2013. Geochemistry of Neoarchean mafic volcanic rocks and late mafic dikes in the Zanhuang Complex, Central Orogenic Belt, North China Craton: implications for geodynamic setting. Lithos 175–176, 193–212.
Faghih, A., Kusky, T.M., Samani, B., 2012. Kinematic analysis of deformed structures in a tectonic melange: a key unit for the manifestation of transpression along the Zagros Suture Zone, Iran. Geological Magazine 149, 1107–1117.
Faure, M., Trap, P., Lin, W., Monié, P., Bruguier, O., 2007. Polyorogenic evolution of the Paleoproterozoic Trans-North China Belt, new insights from the Luliangshan–Hengshan–Wutaishan and Fuping massifs. Episodes 30, 1–12.
Festa, A., Dilek, Y., Pini, G.A., Codegone, G., Ogata, K., 2012. Mechanisms and processes of stratal disruption and mixing in the development of mélanges and broken formations: redefining and classifying mélanges. Tectonophysics 568–569, 7–24.
Fisher, D., Byrne, T., 1987. Structural evolution of underthrusted sediments, Kodiak Islands, Alaska. Tectonics 6, 775–793.
Guo, J.H., O'Brien, P.J., Zhai, M.G., 2002. High–pressure granulites in the Sanggan area, North China Craton: metamorphic evolution, P–T paths and geotectonic significance. Journal of Metamorphic Geology 20, 741–756.
Guo, J.H., Sun, M., Zhai, M.G., 2005. Sm–Nd and SHRIMP U–Pb zircon geochronology of high-pressure granulites in the Sanggan area, North China Craton: timing of Paleoproterozoic continental collision. Journal of Asian Earth Sciences 24, 629–642.
Hashimoto, Y., Kimura, G., 1999. Underplating process from mélange formation to duplexing: examples from the Cretaceous Shimanto Belt, Kii Peninsula, southwest Japan. Tectonics 18, 92–107.
HBGMR (Hebei Bureau of Geology and Mineral Resources), 1996. 1:50000 Regional Geology Survey Report and Geological Map. 11th Geological Team of the Geology Bureau printing house, Hebei, (in Chinese).
HBGMR (Henan Bureau of Geology Mineral Resources), 1989. Regional Geology of Shanxi Province. Geological Publishing House, Beijing (in Chinese).
Hoffman, P.F., 1991. On accretion of granite–greenstone terranes. In: Robert, F., Sheahan, P.A., Green, S.B. (Eds.), Nuna Conference on Greenstone Gold and Crustal Evolution. Geological Association of Canada, Timmins, pp. 32–45.
Kano, K., Nakaji, M., Takeuchi, S., 1991. Asymmetrical mélange fabrics as possible indicators of the convergent direction of plates: a case study from the Shimanto Belt of the Akaishi Mountains, central Japan. Tectonophysics 185, 375–388.
Kimura, G., Mukai, A., 1989. Underplated mélange unit: an example from the Shimanto Belt, Southwest Japan. Earth Monograph II, 697–709 (in Japanese).
Kimura, G., Yamaguchi, A., Hojo, M., Kitamura, Y., Kameda, J., Ujiie, K., Hamada, Y., Hamahashi, M., Hina, S., 2012. Tectonic mélange as fault rock of subduction plate boundary. Tectonophysics 568–569, 25–38.
Kitamura, Y., Kimura, G., 2012. Dynamic role of tectonic mélange during interseismic process of plate boundary mega earthquakes. Tectonophysics 568–569, 39–52.
Kröner, A., Wilde, S.A., Li, J.H., Wang, K.Y., 2005. Age and evolution of a late Archean to early Palaeoproterozoic upper to lower crustal section in the Wutaishan/Hengshan/Fuping terrain of northern China. Journal of Asian Earth Sciences 24, 577–596.
Kröner, A., Wilde, S.A., Zhao, G.C., O'Brien, P.J., Sun, M., Liu, D.Y., Wan, Y.S., Liu, S.W., Guo, J.H., 2006. Zircon geochronology of mafic dykes in the Hengshan Complex of northern China: evidence for late Palaeoproterozoic rifting and subsequent high-pressure event in the North China Craton. Precambrian Research 146, 45–67.
Kusky, T.M., 1989. Accretion of the Archean Slave province. Geology 17, 63–67.
Kusky, T.M., 1990. Evidence for Archean ocean opening and closing in the southern Slave Province. Tectonics 9, 1533–1563.
Kusky, T.M., 2011a. Comparison of results of recent seismic profiles with tectonic models of the North China Craton. Journal of Earth Science 22, 250–259.
Kusky, T.M., 2011b. Geophysical and geological tests of tectonic models of the North China Craton. Gondwana Research 20, 26–35.
Kusky, T.M., Bradley, D.C., 1999. Kinematic analysis of mélange fabrics: examples and applications from the McHugh Complex, Kenai Peninsula, Alaska. Journal of Structural Geology 21, 1773–1797.

Kusky, T.M., Li, J.H., 2003. Paleoproterozoic tectonic evolution of the North China Craton. Journal of Asian Earth Sciences 22, 383–397.
Kusky, T.M., Li, J.H., 2010. Origin and emplacement of ophiolites of the Central Orogenic Belt, North China Craton. Journal of Earth Science 21, 744–781.
Kusky, T.M., Polat, A., 1999. Growth of granite–greenstone terranes at convergent margins, and stabilization of Archean cratons. Tectonophysics 305, 43–73.
Kusky, T.M., Santosh, M., 2009. The Columbia connection in North China. In: Reddy, S.M., Mazumder, R., Evans, D., Collins, A.S. (Eds.), Paleoproterozoic Supercontinents and Global Evolution. Geological Society of London, Special Publication, 323, pp. 49–71.
Kusky, T.M., Bradley, D.C., Haeussler, P., Karl, S., 1997. Controls on accretion of flysch and mélange belts at convergent margins: evidence from The Chugach Bay thrust and Iceworm mélange, Chugach Terrane, Alaska. Tectonics 16, 855–878.
Kusky, T.M., Li, J.H., Tucker, R.T., 2001. The Archean Dongwanzi ophiolite complex, North China Craton: 2.505 billion year old oceanic crust and mantle. Science 292, 1142–1145.
Kusky, T.M., Li, Z.H., Glass, A., Huang, H.A., 2004. Archean ophiolites and ophiolite fragments of the North China Craton. In: Kusky, T.M. (Ed.), Precambrian Ophiolites and Related Rocks. Developments in Precambrian Geology, 13. Elsevier, Amsterdam, pp. 223–274.
Kusky, T.M., Windley, B.F., Zhai, M.G., 2007a. Tectonic evolution of the North China Block: from orogen to craton to orogen. In: Zhai, M.G., Windley, B.F., Kusky, T.M., Meng, Q.R. (Eds.), Mesozoic Sub-continental Lithospheric Thinning Under Eastern Asia. Geological Society of London, Special Publication, 280, pp. 1–34.
Kusky, T.M., Li, J.H., Santosh, M., 2007b. The Paleoproterozoic North Hebei Orogen: North China Craton's collisional suture with Columbia supercontinent. In: Zhai, M.G., Xiao, W.J., Kusky, T.M., Santosh, M. (Eds.), Tectonic Evolution of China and Adjacent Crustal Fragments. Gondwana Research, 12, pp. 4–28.
Kusky, T.M., Stern, R.J., Dewey, J.F., 2013. Secular changes in geologic and tectonic process. Gondwana Research 24, 451–452.
Li, J.H., Kusky, T.M., 2007. A Late Archean foreland fold and thrust belt in the North China Craton: implications for early collisional tectonics. In: Zhai, M.G., Xiao, W.J., Kusky, T.M., Santosh, M. (Eds.), Tectonic Evolution of China and Adjacent Crustal Fragments. Gondwana Research, 12, pp. 47–66.
Li, J.H., Qian, X.L., Huang, X.N., Liu, S.W., 2000a. The tectonic framework of the basement of North China Craton and its implication for the early Precambrian cratonization. Acta Petrologica Sinica 16, 1–10 (in Chinese with English abstract).
Li, J.H., Kröner, A., Qian, X.L., O'Brien, P., 2000b. The tectonic evolution of early Precambrian high-pressure granulite belt, North China Craton (NCC). Acta Geological Sinica 274, 246–256 (in Chinese with English abstract).
Li, T.S., Zhai, M.G., Peng, P., Chen, L., Guo, J.H., 2010. Ca. 2.5 billion year old coeval ultramafic–mafic and syenitic dykes in Eastern Hebei: implications for cratonization of the North China Craton. Precambrian Research 180, 143–155.
Lin, S., Percival, J.A., Skulski, T., 1996. Structural constraints on the tectonic evolution of a late Archean greenstone belt in the northeastern Superior Province, northern Quebec (Canada). Tectonophysics 265, 151–167.
Liu, S., Pan, Y., Li, J., Li, Q., 2004. Archean geodynamics in the Central Zone, North China Craton: constraints from geochemistry of two contrasting series of granitoids in the Fuping and Wutaishan complexes. Precambrian Research 130, 229–249.
Liu, S., Pan, Y., Xie, Q., Zhang, J., Li, Q., Yang, B., 2005. Geochemistry of the Paleoproterozoic Nanying Granitoid Gneisses: constraints on the tectonic setting of the Central Zone, North China Craton. Journal of Asian Earth Sciences 24, 643–658.
Liu, S., Zhao, G., Wilde, S.A., Shu, G., Sun, M., Li, Q., Tian, W., Zhang, J., 2006. Th–U–Pb monazite geochronology of the Luliang and Wutai Complexes: constraints on the tectonothermal evolution of the Trans-North China Orogen. Precambrian Research 148, 205–224.
Liu, Y.S., Gao, S., Hu, Z.C., Gao, C.G., Zong, K.Q., Wang, D.B., 2009. Continental and oceanic crust recycling-induced melt-peridotite interactions in the Trans-North China Orogen: U–Pb dating, Hf isotopes and trace elements in zircons of mantle xenoliths. Journal of Petrology 51, 537–571.
Liu, Y.S., Hu, Z.C., Zong, K.Q., Gao, C.G., Gao, S., Xu, J., Chen, H.H., 2010. Reappraisement and refinement of zircon U–Pb isotope and trace element analyses by LA–ICP–MS. Chinese Science Bulletin 55, 1535–1546.
Ludwig, K.R., 2003. User's manual for Isoplot/Ex rev. 3.00: a geochronological toolkit for Microsoft Excel. Berkeley Geochronology Center, Special Publication, 4, p. 70.
Meng, Q.R., Wei, H.H., Qu, Y.Q., Ma, S.X., 2011. Stratigraphic and sedimentary records of the rift to drift evolution of the northern North China craton at the Paleo- to Mesoproterozoic transition. Gondwana Research 20, 205–218.
Moyen, J.F., van Hunen, J., 2012. Short term episodicity of Archean plate tectonics. Geology 40, 451–454.
Needham, D.T., 1987. Asymmetric extensional structures and their implication for the generation of mélanges. Geological Magazine 124, 311–318.
Needham, D.T., Mackenzie, J.S., 1988. Structural evolution of the Shimanto belt accretionary complex in the area of the Gokase River, Kyushu, SW Japan. Journal of the Geological Society of London 145, 85–94.
Nutman, A.P., Wan, Y.S., Du, L.L., Friend, C.R.L., Dong, C.Y., Xie, H.Q., Wang, W., Sun, H.Y., Liu, D.Y., 2011. Multistage late Neoarchean crustal evolution of the North China Craton, eastern Hebei. Precambrian Research 189, 43–65.
Onishi, C.T., Kimura, G., 1995. Change in fabric of mélange in the Shimanto Belt, Japan: change in relative convergence? Tectonics 14, 1273–1289.
Paterson, S.R., Tobisch, O.T., 1988. Using pluton ages to date regional deformations: problems with commonly used criteria. Geology 16, 1108–1111.
Paterson, S.R., Vernon, R.H., 1995. Bursting the bubble of ballooning plutons: a return to nested diapirs emplaced by multiple processes. Geological Society of America Bulletin 107, 1356–1380.
Peng, P., Zhai, M.G., Guo, J.H., Kusky, T.M., Zhao, T.P., 2007. Nature of mantle source contributions and crystal differentiation in the petrogenesis of the 1.78 Ga mafic dykes in the central North China craton. Gondwana Research 12, 29–46.
Polat, A., Casey, J.F., 1995. A structural record of the emplacement of the Pozanti–Karsanti ophiolite onto the Menderes–Taurus block in the late Cretaceous, eastern Taurides, Turkey. Journal of Structure Geology 17, 1673–1688.
Polat, A., Kerrich, R., 1999. Formation of an Archean tectonic mélange in the Schreiber–Hemlo greenstone belt, Superior Province, Canada: implication for Archean subduction–accretion process. Tectonics 18, 733–755.
Polat, A., Kerrich, R., Wyman, D.A., 1998. The late Archean Schreiber–Hemlo and White River Dayohessarah greenstone belts, Superior Province: collages of oceanic plateaus, oceanic arcs, and subduction–accretion complexes. Tectonophysics 289, 295–326.
Polat, A., Kusky, T.M., Li, J.H., Fryer, B., Kerrich, R., Patrick, K., 2005. Geochemistry of the Late Archean (ca. 2.55–2.50 Ga) volcanic and ophiolitic rocks in the Wutaishan Greenstone Belt, Central Orogenic Belt, North China Craton: implications for geodynamic setting and continental growth. Geological Society of America Bulletin 117, 1387–1399.
Polat, A., Li, J.H., Fryer, B., Kusky, T.M., Gagnon, J., Zhang, S., 2006a. Geochemical characteristics of the Neoarchean (2800–2700 Ma) Taishan greenstone belt, North China Craton: evidence for plume–craton interaction. Chemical Geology 230, 60–87.
Polat, A., Herzberg, C., Munker, C., Rodgers, R., Kusky, T.M., Li, J.H., Fryer, B., Delany, J., 2006b. Geochemical and petrological evidence for a suprasubduction zone origin of Neoarchean (ca. 2.5 Ga) peridotites, Central Orogenic Belt, North China Craton. Geological Society of America Bulletin 118, 771–784.
Santosh, M., 2010. Assembling North China Craton within the Columbia supercontinent: the role of double-sided subduction. Precambrian Research 178, 149–167.
Şengör, A.M.C., Natalin, B.A., 1996. Paleotectonics of Asia: fragment of a synthesis. In: Yin, A., Harrison, T.M. (Eds.), The Tectonics of Asia. Cambridge University Press, New York, pp. 486–640.
Shen, Q.H., Xu, H.F., Zhang, Z.Q., 1992. The Early Precambrian Granulites in China. Geological Publishing House, Beijing (in Chinese).
Shen, Q., Zhang, Z.Q., Geng, Y.S., 1994. The petrology, geochemistry, and isotopic age dating of Dadonggou garnet-bearing granulite, Northwest Hebei. In: Qian, X., Wang, R. (Eds.), The Geological Evolution of North China Granulite Belt, 120. Beijing Seismological Press, p. 129 (in Chinese with English abstract).
Singleton, J.S., Cloos, M., 2012. Kinematic analysis of mélange fabrics in the Franciscan Complex near San Simeon, California: evidence for sinistral slip on the Nacimiento fault zone? Lithosphere 5, 179–188.
Stern, R.J., 2007. When and how did plate tectonics begin? Theoretical and empirical considerations. Chinese Science Bulletin 52, 578–591.
Taira, A., Katto, J., Tashiro, M., Okamura, M., Kodama, K., 1988. The Shimanto Belt in Shikoku, Japan–evolution of Cretaceous to Miocene accretionary prism. Modern Geology 12, 5–46.
Taira, A., Pickering, K.T., Windley, B.F., Soh, W., 1992. Accretion of Japanese island arcs and implications for the origin of Archean greenstone belts. Tectonics 11, 1224–1244.
Trap, P., Faure, M., Lin, W., Monié, P., 2007. Late Palaeoproterozoic (1900–1800 Ma) nappe stacking and polyphase deformation in the Hengshan–Wutaishan area: implication for the understanding of the Trans-North China Belt, North China Craton. Precambrian Research 156, 85–106.
Trap, P., Faure, M., Lin, W., Bruguier, O., Monié, P., 2008. Contrasted tectonic styles for the Paleoproterozoic evolution of the North China Craton: evidence for a 2.1 Ga thermal and tectonic event in the Fuping Massif. Journal of Structural Geology 30, 1109–1125.
Trap, P., Faure, M., Lin, W., Monié, P., Meffre, S., Melleton, J., 2009a. The Zanhuang Massif, the second and eastern suture zone of the Paleoproterozoic Trans-North China Orogen. Precambrian Research 172, 80–98.
Trap, P., Faure, M., Lin, W., Meffre, S., 2009b. The Luliang Massif: a key area for the understanding of the Palaeoproterozoic Trans-North China Belt, North China Craton. Journal of the Geological Society Special Publication 33, 99–125.
Trap, P., Faure, M., Lin, W., Breton, N.L., Monié, P., 2012. Paleoproterozoic tectonic evolution of the Trans-North China Orogen: toward a comprehensive model. Precambrian Research 222–223, 191–211.
Ujiie, K., 2002. Evolution and kinematics of an ancient décollement zone, mélange in the Shimanto accretionary complex of Okinawa Island, Ryukyu Arc. Journal of Structural Geology 24, 937–955.
Vernon, R.H., Paterson, S.R., Geary, E.E., 1989. Evidence for syntectonic intrusion of plutons in the Bear Mountains fault zone, California. Geology 17, 723–726.
Wakabayashi, J., 1996. Tectono-metamorphic impact of a subduction–transform transition and implications for interpretation of orogenic belts. International Geology Review 38, 979–994.
Wakabayashi, J., Dilek, Y., 2011. Introduction: characteristics and tectonic settings of mélanges, and their significance for societal and engineering problems. In: Wakabayashi, J., Dilek, Y. (Eds.), Mélanges: Processes of Formation and Societal Significance. Geological Society of America Special Paper, 480, pp. v–x.
Waldron, J.W.F., Turner, D., Stevens, K.M., 1988. Stratal disruption and development of mélange, western Newfoundland: effect of high fluid pressure in an accretionary terrain during ophiolite emplacement. Journal of Structural Geology 10, 861–873.
Wang, Z.H., 2009. Tectonic evolution of the Hengshan–Wutai–Fuping complexes and its implication for the Trans-North China Orogen. Precambrian Research 170, 73–87.
Wang, K.Y., Li, J.L., Hao, J., Li, J.H., Zhou, S.P., 1996. The Wutaishan orogenic belt within the Shanxi Province, northern China: a record of late Archean collision tectonics. Precambrian Research 78, 95–103.
Wang, Y.J., Fan, W.M., Zhang, Y., Guo, F., 2003. Structural evolution and $^{40}Ar/^{39}Ar$ dating of the Zanhuang metamorphic domain in the North China Craton: constraints on Paleoproterozoic tectonothermal overprinting. Precambrian Research 122, 159–182.
Wang, Z.H., Wilde, S.A., Wang, K.Y., Yu, L.J., 2004. A MORB–arc basalt–adakite association in the 2.5 Ga Wutai greenstone belt: Late Archean magmatism and crustal growth in the North China Craton. Precambrian Research 131, 323–343.

Wang, Y.J., Zhao, G.C., Cawood, P.A., Fan, W.M., Peng, T.P., Sun, L.H., 2008. Geochemistry of Paleoproterozoic (1770 Ma) mafic dikes from the Trans-North China Orogen and tectonic implications. Journal of Asian Earth Sciences 33, 61–77.
Wang, Z.H., Wilde, S.A., Wan, J.L., 2010. Tectonic setting and significance of 2.3–2.1 Ga magmatic events in the Trans-North China Orogen: new constraints from the Yanmenguan mafic–ultramafic intrusion in the Hengshan–Wutai–Fuping area. Precambrian Research 178, 27–42.
Wilde, S.A., Zhao, G.C., 2005. Archean to Paleoproterozoic evolution of the North China Craton. Journal of Asian Earth Sciences 24, 519–522.
Wilde, S.A., Zhao, G.C., Sun, M., 2002. Development of the North China Craton during the Late Archaean and its final amalgamation at 1.8 Ga: some speculations on its position within a global Palaeoproterozoic Supercontinent. Gondwana Research 5, 85–94.
Windley, B.F., 1993. Uniformitarianism today: plate tectonics is the key to the past. Journal of the Geological Society 150, 7–19.
Xiao, L.L., Wang, G.D., 2011. Zircon U–Pb dating of metabasic rocks in the Zanhuang metamorphic complex and its geological significance. Acta Petrologica et Mineralogica 30, 781–794 (in Chinese with English abstract).
Yang, C.H., Du, L.L., Ren, L.D., Song, H.X., Wan, Y.S., Xie, H.Q., Geng, Y.S., 2013. Delineation of the ca. 2.7 Ga TTG gneisses in the Zanhuang Complex, North China Craton and its geological implications. Journal of Asian Earth Sciences 72, 178–189.
Zhai, M.G., 2004. 2.1–1.7 Ga geological event group and its geotectonic significance. Acta Petrologica Sinica 20, 1343–1354.
Zhai, M.G., Liu, W.J., 2003. Palaeoproterozoic tectonic history of the North China Craton: a review. Precambrian Research 122, 183–199.
Zhai, M.G., Santosh, M., 2011. The early Precambrian odyssey of the North China Craton: a synoptic overview. Gondwana Research 20, 6–25.
Zhang, J., Zhao, G.C., Li, S.Z., Sun, M., Liu, S.W., Wilde, S.A., Kröner, A., Yin, C.Q., 2007. Deformation history of the Hengshan Complex: Implications for the tectonic evolution of the Trans North China Orogen. Journal of Structural Geology 29, 933–949.
Zhao, G.C., 2001. Paleoproterozoic assembly of the North China Craton. Geological Magazine 138, 87–91.
Zhao, G.C., Cawood, P.A., 2012. Precambrian geology of China. Precambrian Research 222–223, 13–54.
Zhao, G.C., Wilde, S.A., Cawood, P.A., Lu, L.Z., 1998. Thermal evolution of basement rocks from the eastern part of the North China Craton and its bearing on tectonic setting. International Geology Review 40, 706–721.
Zhao, G.C., Wilde, S.A., Cawood, P.A., Lu, L.Z., 1999a. Thermal evolution of two textural types of mafic granulites in the North China Craton: evidence for both mantle plume and collisional tectonics. Geological Magazine 136, 223–240.
Zhao, G.C., Wilde, S.A., Cawood, P.A., Lu, L.Z., 1999b. Tectonothermal history of the basement rocks in the western zone of the North China Craton and its tectonic implications. Tectonophysics 310, 37–53.
Zhao, G.C., Cawood, P.A., Wilde, S.A., Lu, L.Z., 2000a. Metamorphism of basement rocks in the Central Zone of the North China Craton: implications for Paleoproterozoic tectonic evolution. Precambrian Research 103, 55–88.
Zhao, G.C., Wilde, S.A., Cawood, P.A., Lu, L.Z., 2000b. Petrology and P–T–t path of the Fuping mafic granulites: implications for tectonic evolution of the central zone of the North China Craton. Journal of Metamorphic Petrology 18, 375–391.
Zhao, G.C., Wilde, S.A., Cawood, P.A., Sun, M., 2001a. Archean blocks and their boundaries in the North China Craton: lithological, geochemical, structural and P–T path constraints and tectonic evolution. Precambrian Research 107, 45–73.
Zhao, G.C., Wilde, S.A., Cawood, P.A., Lu, L.Z., 2001b. High-pressure granulites (retrograded eclogites) from the Hengshan Complex, North China Craton: petrology and tectonic implications. Journal of Petrology 42, 1141–1170.
Zhao, G.C., Cawood, P.A., Wilde, S.A., Sun, M., Lu, L.Z., 2002a. Metamorphism of basement rocks in the Central Zone of the North China Craton: implications for Paleoproterozoic tectonic evolution. Precambrian Research 103, 55–88.
Zhao, G.C., Wilde, S.A., Cawood, P.A., Sun, M., 2002b. SHRIMP U–Pb zircon ages of the Fuping Complex: implications for late Archean to Paleoproterozoic accretion and assembly of the North China Craton. American Journal of Science 302, 191–226.
Zhao, G.C., Sun, M., Wilde, S.A., Guo, J.H., 2004. Late Archean to Palaeoproterozoic evolution of the Trans-North China Orogen: insights from synthesis of existing data from the Hengshan–Wutai–Fuping belt. In: Malpas, J., Fletcher, C.J.N., Ali, J.R., Aitchison, J.C. (Eds.), Aspects of the Tectonic Evolution of China. Geological Society of London, Special Publication, 226, pp. 27–55.
Zhao, G.C., Sun, M., Wilde, S., Li, S.Z., 2005. Late Archean to Paleoproterozoic evolution of the North China Craton: key issues revisited. Precambrian Research 136, 177–202.
Zhao, G.C., Kröner, A., Wilde, S.A., Sun, M., Li, S.Z., Li, X.P., Zhang, J., Xia, X.P., He, Y.H., 2007. Lithotectonic elements and geological events in the Hengshan–Wutai–Fuping belt: a synthesis and implications for the evolution of the Trans-North China Orogen. Geological Magazine 144, 753–775.
Zhao, G.C., Wilde, S.A., Zhang, J., 2010. New evidence from seismic imaging for subduction during assembly of the North China craton: comment. Geology 38, 206.
Zheng, T.Y., Zhao, L., Zhu, R.X., 2009. New evidence from seismic imaging for subduction during assembly of the North China Craton. Geology 37, 395–398.